

博士論文（要約）

**Investigation of the role of prostaglandin D<sub>2</sub>  
in tumor microenvironment**

（腫瘍微小環境におけるプロスタグランジン D<sub>2</sub> の役割解明）

大森 啓介

# Index

Chapter 1 Introduction.....	5
1-1 Tumor growth and metastasis.....	5
1-2 Tumor microenvironment.....	5
1-2-1 Endothelial cells .....	6
1-2-2 Immune cells.....	6
1-3 Prostaglandins and tumor microenvironment.....	7
1-4 PGD <sub>2</sub> .....	8
1-5 PGD <sub>2</sub> and tumor microenvironment.....	9
1-6 Aim.....	9
Chapter 2 Role of L-PGDS-derived PGD <sub>2</sub> in tumor growth.....	12
2-1 Aim of Chapter 2 .....	12
2-2 Induction of L-PGDS in tumor ECs .....	13
2-2-1 Expression of angiogenesis-related factors in ECs of melanoma .....	13
2-2-2 Expression of L-PGDS in LLC and 4T1 ECs.....	15
2-2-3 Localization of L-PGDS in tumor .....	16
2-2-4 Localization of L-PGDS in human tumor .....	18
2-2-5 Expression of L-PGDS in melanoma supernatant-treated EC.....	19

2-2-6 Effect of IL-1 or TNF- $\alpha$ antagonist on expression of L-PGDS in EC.....	20
2-2-7 Effect of tyrosine kinase or COX inhibitor on expression of L-PGDS in EC.....	21
2-2-8 PGD <sub>2</sub> production in melanoma supernatant-treated EC .....	22
2-3 Role of endothelial L-PGDS in tumor growth .....	24
2-3-1 Melanoma or LLC growth in WT and L-PGDS deficient mice .....	24
2-3-2 PGD <sub>2</sub> content in WT and L-PGDS <sup>-/-</sup> mice tumor .....	25
2-3-3 Effect of DP agonist on tumor growth.....	26
2-3-4 Tumor growth in CRTH2 deficient mice .....	27
2-3-5 Effect of PGD <sub>2</sub> on cultured tumor cell proliferation and survival.....	28
2-3-6 Tumor growth in WT or L-PGDS <sup>-/-</sup> bone marrow transplanted mice .....	29
2-3-7 Tumor growth in endothelial-specific L-PGDS deficient mice.....	30
2-4 Morphological analysis of tumor.....	31
2-4-1 HE staining of tumor .....	31
2-4-2 Proliferative rate of tumor .....	33
2-4-3 Apoptotic rate of tumor .....	34
2-5 Role of endothelial L-PGDS in tumor vessels .....	36
2-5-1 Hypoxic region in tumor.....	36
2-5-2 Angiogenesis and vascular permeability in tumor .....	38
2-5-3 Vessel maturation in tumor.....	41

2-5-4 Functional vessels in tumor .....	44
2-5-5 Endothelial-to-mesenchymal transition in tumor .....	46
2-5-6 mRNA expression of EndMT markers in tumor ECs.....	49
2-5-7 mRNA expression of EndMT markers in melanoma supernatant-treated EC ....	50
2-5-8 Immune cell infiltration in tumor .....	51
2-6 Role of L-PGDS in vascular permeability and angiogenesis in mice inflammation model .....	53
2-6-1 Role of L-PGDS in ear vascular hyper-permeability .....	53
2-6-2 L-PGDS localization in mice ear.....	55
2-6-3 Role of L-PGDS in cornea angiogenesis.....	56
2-7 Discussion of chapter 2 .....	57
Chapter 3 Role of PGD <sub>2</sub> in tumor metastasis .....	61
Chapter 4 Total discussion .....	62
Chapter 5 Abstract.....	63
Chapter 6 Material and Methods .....	64
Chapter 7 Reference .....	65
Acknowledgement.....	70

# Chapter 1 Introduction

## 1-1 Tumor growth and metastasis

Tumor, including its malignant form, cancer, is one of the major causes of death all over the world. Every year, about 8 million people were estimated to die of tumor (1), and the number is still increasing. Tumor cells arise from carcinogenic and mutagenic stimuli, such as radiation, viral infection, and also chronic inflammation. Tumor cells abnormally proliferate at the primary lesion, and metastasize to distant organs via blood/lymph vessels. Since the risk of metastasis correlated to primary tumor size and tumor metastasis are responsible for approximately 90% of all tumor-related deaths (2), elucidating the precise mechanisms of tumor growth and metastasis are urgently needed for effective tumor therapy.

## 1-2 Tumor microenvironment

To clarify the precise mechanisms of tumor growth and metastasis, I here focused on tumor microenvironment, which was composed of non-tumor cells. Tumor cells produce various cytokines/chemokines/growth factors and induce inflammatory reactions of surrounding stromal cells. Tumor cells manipulate the tumor environment to acquire adequate nutrients/oxygen and also avoid host immunosurveillance. The main cell types in the tumor microenvironment were endothelial cells and immune cells (Fig. 1), as described below.

### **1-2-1 Endothelial cells**

To receive enough nutrients and oxygen, tumor cells produce cytokines and/or growth factors to stimulate the formation of new vessels, by a process called angiogenesis (3). Tumor vessels mainly comprise tumor endothelial cells (ECs), which possess completely different characteristics and functions compared to normal ECs. ECs in tumor have abnormal structures such as fenestrations and widened intercellular junctions (4), constructing hyper-permeable and angiogenic vessels. They also have a high proliferation rate and migration capability (5). Some tumor ECs become cancer-associated fibroblasts by endothelial-to-mesenchymal transition (EndMT) (6), producing large amounts of tumorigenic cytokines and growth factors (7). Recent studies have identified several molecules that are specifically upregulated in human ECs in the colon (8), lung, bladder, and breast cancer (9). Several studies have also reported the morphological characteristics and antigen markers of ECs in tumor. Since tumor vessels are indispensable for tumor growth and metastasis, normalizing and reducing tumor vessels can be developed into an anti-tumor therapy. However, it is still unclear how tumors modulate the functional characteristics of tumor ECs.

### **1-2-2 Immune cells**

Host immune system plays an important role in detecting and rejecting tumor cells. In particular, Natural killer (NK) cells, CD8<sup>+</sup> T cells, and T helper 1 (Th1) cells reject primary and metastatic tumor cells. NK and CD8<sup>+</sup> T cells directly kill various types of tumor cells by secreting cytotoxic products (perforin and granzymes) or cytokines [tumor

necrosis factor- $\alpha$  (TNF- $\alpha$ ) and interferon gamma (IFN $\gamma$ )] (10, 11). Th1 cells also have IFN $\gamma$ -dependent cytotoxic effects in human tumor (12). To avoid these host immunosurveillance, tumor cells induce the infiltration of immunosuppressive cells such as myeloid-derived suppressor cells (MDSCs), T regulatory (Treg) cells, tumor-associated macrophages, and Th2 cells. In previous reports using mice tumor models, these cells produce immunosuppressive cytokines (i.e. transforming growth factor  $\beta$ , IL-4, IL-10, IL-12, IL-13, or iNOS), leading to inactivate the host immune responses (13, 14). Recently, several drugs activating CD8<sup>+</sup> T cells have been proposed (15, 16), and provide significant impact on the strategies of cancer treatment. Therefore, many researchers are now focusing on the immune cells in tumor microenvironment.

### **1-3 Prostaglandins and tumor microenvironment**

Prostaglandins (PGs) are lipid autacoids synthesized from cell membrane-derived arachidonic acid. Arachidonic acid is first converted to PGH<sub>2</sub> by an enzyme cyclooxygenase (COX), and then to PGs by each PG synthase (Fig. 2). PGs maintain the homeostasis in the resting state by regulating the kidney blood flow and protecting gastric mucosa. During inflammation, PGs are abundantly produced and worsen the pathologies of various inflammatory diseases (17). Since PGs has central role in modulating inflammation, several studies focused on their role in tumor microenvironment. Epidemiologic studies revealed that routine use of COX-2 inhibitors (known as NSAIDs) inhibited the progression and prognosis of human colon, breast, prostate, and lung cancer (18, 19). In addition, another study revealed that expression of COX-2 in human colon cancer cells increased

their metastatic potential (20), suggesting its contribution in tumor metastasis. There are mainly 5 PGs, PGE<sub>2</sub>, PGD<sub>2</sub>, PGF<sub>2α</sub>, PGI<sub>2</sub>, and thromboxane A<sub>2</sub> (TXA<sub>2</sub>), which have distinct physiological/pathophysiological function (Fig. 2). PGE<sub>2</sub> has been well studied and recognized as important exacerbating factor in inflammatory diseases. In terms of tumor microenvironment, PGE<sub>2</sub> acts on tumor vessels and enhances angiogenesis, leading to promote the growth of mice colorectal (21) and breast cancer (22). Other group also revealed that PGE<sub>2</sub> recruited MDSCs, leading to promote colorectal tumor growth and metastasis in mice (23). Inhibition of PGE<sub>2</sub> signal shows significant reduction of mice lung metastasis (24). However, there are few studies focusing on other PGs in tumor microenvironment.

### **1-4 PGD<sub>2</sub>**

PGD<sub>2</sub> is one of major PGs that are synthesized by COX and lipocalin-type or hematopoietic PGD synthase (L-PGDS and H-PGDS, respectively). L-PGDS is expressed mainly in oligodendrocytes and epithelial cells in choroid plexus (25), regulating physiological sleep (26) and allodynia response (27). Recent studies also reported that expression of L-PGDS was induced by blood shear stress in ECs (28), though its physiological and/or pathological roles remain unknown. In contrast, H-PGDS is expressed in immune cells such as mast cells/Th2 cells and also in endothelial/epithelial cells. Previous reports showed that H-PGDS-derived PGD<sub>2</sub> regulated allergic diseases such as asthma (29) and food allergy (30).

PGD<sub>2</sub> shows its bioactivity via two G-protein-coupled receptors (GPCRs), DP and CRTH2. Some researchers reported that PGD<sub>2</sub>-DP signaling abrogated the pathologies of mice skin allergy and asthma by attenuating the activities of dendritic and Treg cells (31, 32). Our group also revealed its anti-inflammatory role in several mice pathological models such as acute lung injury and skin inflammation (33, 34). In these reports, PGD<sub>2</sub> acted on endothelial DP, leading to enhance endothelial barrier and attenuate vascular permeability. In contrast, previous studies also revealed the pro-inflammatory role of PGD<sub>2</sub>-CRTH2 signaling in the inflammatory diseases such as asthma and chronic allergic skin inflammation (29, 35). In these studies, PGD<sub>2</sub> induced the chemotaxis of CRTH2-positive eosinophils and Th2 cells, leading to amplify the inflammatory loop in the lesion. As mentioned above, PGD<sub>2</sub> has multiple roles in regulating inflammatory diseases and its action is highly dependent on the localizations of its synthases and receptors.

.

#### **1-5 PGD<sub>2</sub> and tumor microenvironment**

本章の内容は、学術雑誌論文として出版する計画があるため公表できない。

5年以内に出版予定

#### **1-6 Aim**

本章の内容は、学術雑誌論文として出版する計画があるため公表できない。

5年以内に出版予定

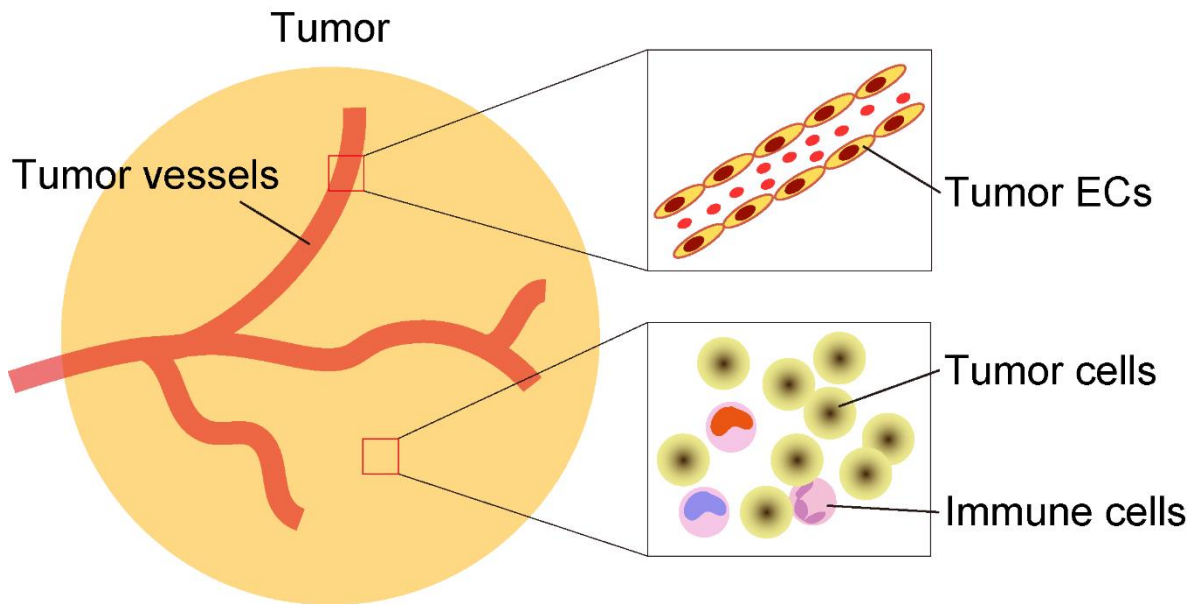


**Figure 1 Tumor cells and tumor microenvironment**

Tumor microenvironment is mainly composed of tumor ECs and immune cells. Tumor cells manipulate this microenvironment to acquire adequate nutrients/oxygen and also avoid host immunosurveillance.

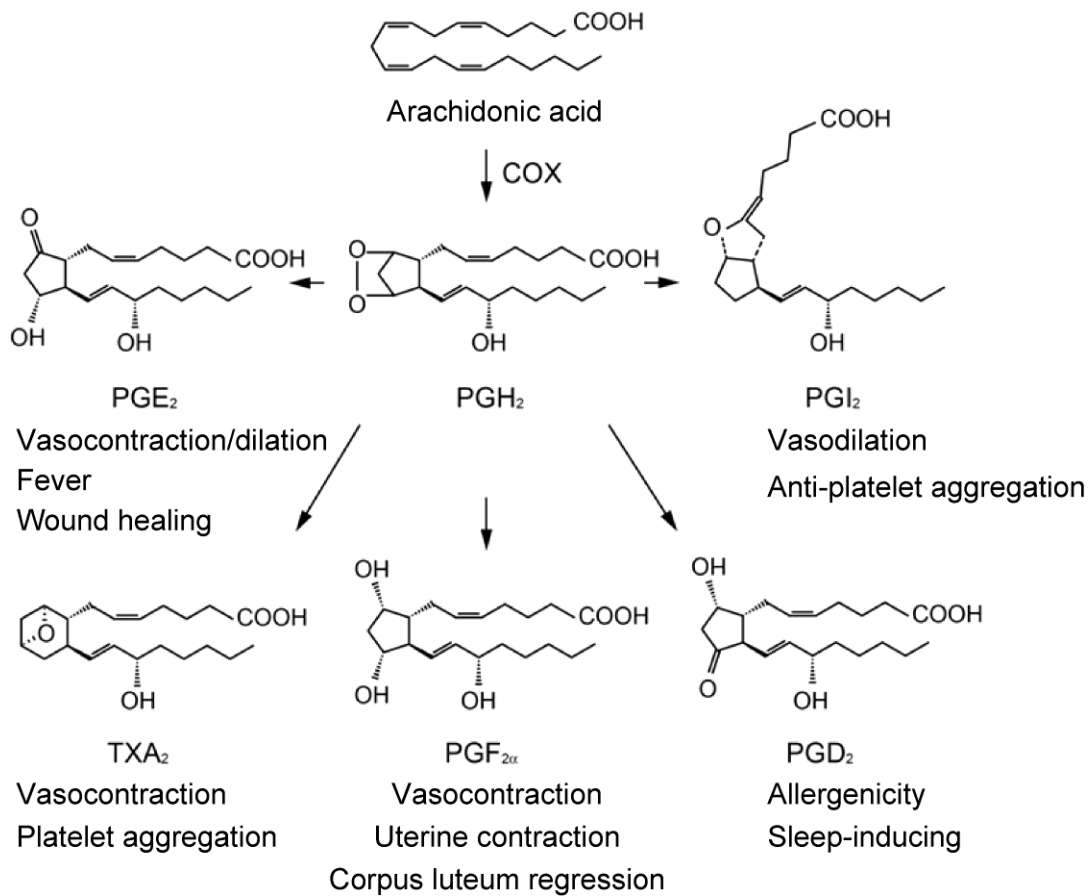


**Figure 2 Synthetic pathway of PG**

PGH<sub>2</sub> is synthesized via enzyme reaction of COX from cell membrane-derived arachidonic acid. PGH<sub>2</sub> is converted to PGE<sub>2</sub>, PGD<sub>2</sub>, PGF<sub>2α</sub>, PGI<sub>2</sub>, and TXA<sub>2</sub> via each PG synthase which exerts various physiological functions.

# **Chapter 2 Role of L-PGDS-derived PGD<sub>2</sub> in tumor growth**

## **2-1 Aim of Chapter 2**

In this chapter, I investigated the contribution of L-PGDS-derived PGD<sub>2</sub> in tumor growth. In the resting condition, expression of L-PGDS was hardly observed in ECs and immune cells, which create the tumor microenvironment. However, *in vitro* experiments showed the induction of L-PGDS in ECs by abnormal blood flow (28). Since tumor ECs was consistently exposed to abnormal blood flow, I here speculated that L-PGDS might be expressed in tumor ECs and regulate the tumor growth by producing PGD<sub>2</sub>.

## **2-2 Induction of L-PGDS in tumor ECs**

### **2-2-1 Expression of angiogenesis-related factors in ECs of melanoma**

Tumor ECs were isolated from subcutaneously-implanted B16F1 melanoma and its mRNA expression levels of angiogenesis-related factors were determined. Consistent with previous reports (36, 37), expression of COX-2 was upregulated, and that of intercellular adhesion molecule-1 (ICAM-1) was downregulated in tumor ECs, as compared to ECs in normal tissues (mouse lung ECs; MLECs) (Fig. 3). Expression levels of IL-1 $\beta$ , IL-4, H-PGDS, prostaglandin I synthase (PGIS), matrix metalloproteinase 9 (MMP9), and vascular cell adhesion molecule-1 (VCAM-1) were 2-8 fold higher in melanoma ECs than in MLECs. Interestingly, the expression of L-PGDS was markedly increased (about 15-fold; Fig. 3).

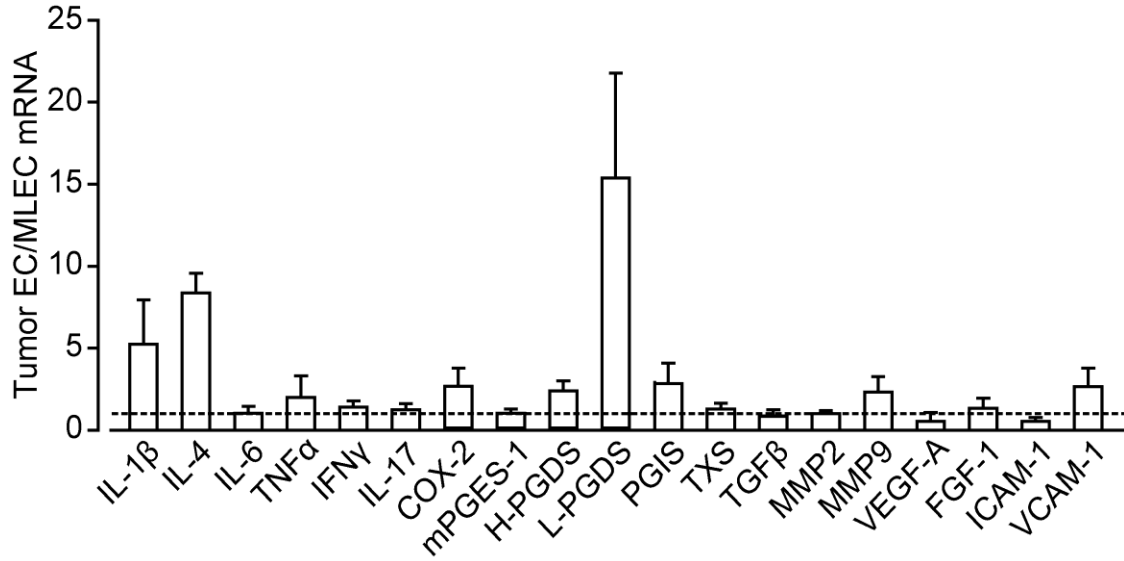


**Figure 3 Marked increase of mRNA expression of L-PGDS in melanoma ECs**

Relative expression of angiogenesis-related factors in ECs of melanoma compared to that in MLECs (n = 5). Dot line indicates equal mRNA expression of tumor ECs and MLECs. Data are presented as means  $\pm$  SEM.

### 2-2-2 Expression of L-PGDS in LLC and 4T1 ECs

mRNA expression of L-PGDS in tumor ECs was also observed using other tumor cell lines, lewis lung carcinoma (LLC) and 4T1 breast tumor cells. Compared to other prostaglandin synthases (about 2 to 4-fold; Fig. 4A), mRNA expression of L-PGDS was markedly increased (about 10-fold, Fig. 4A) in LLC tumor ECs. The expression was also increased in 4T1 ECs (about 4-fold, Fig. 4B).

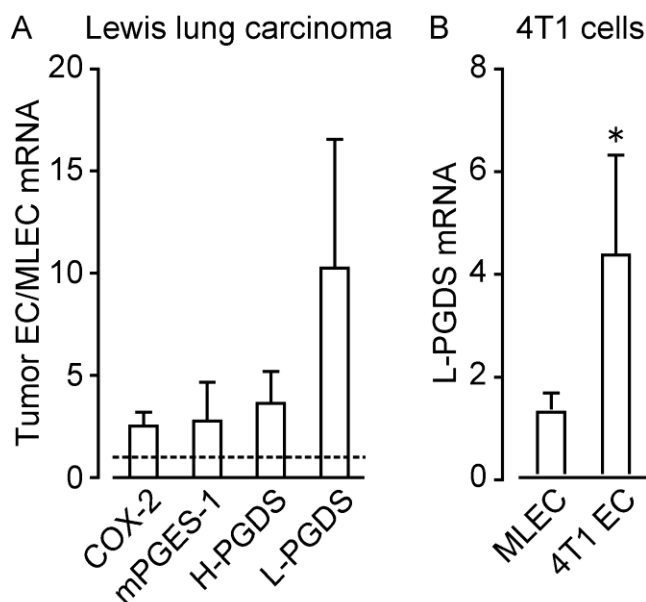


**Figure 4** Marked increase of mRNA expression of L-PGDS in LLC and 4T1 ECs

(A) Relative expression of prostaglandin synthases in ECs of LLC compared to that in MLECs (n = 5). (B) Relative expression of L-PGDS in ECs of MLEC or 4T1 in BALB/c mice (n = 6). \* Significantly different from the results in MLEC group at  $p < 0.05$ . Data are presented as means  $\pm$  SEM.

### **2-2-3 Localization of L-PGDS in tumor**

Immunofluorescence staining showed that L-PGDS (red) was specifically localized to CD31 (green) positive tumor ECs (Fig. 5A, upper panels) in B16F1 melanoma. In detail, L-PGDS was localized in granular endoplasmic reticulum, adjacent to the cell nucleus as previously described in oligodendrocytes (25) (Fig. 5A, lower panels). The protein expression of L-PGDS in tumor ECs was also detected in 4T1 tumor ECs. (Fig. 5B).

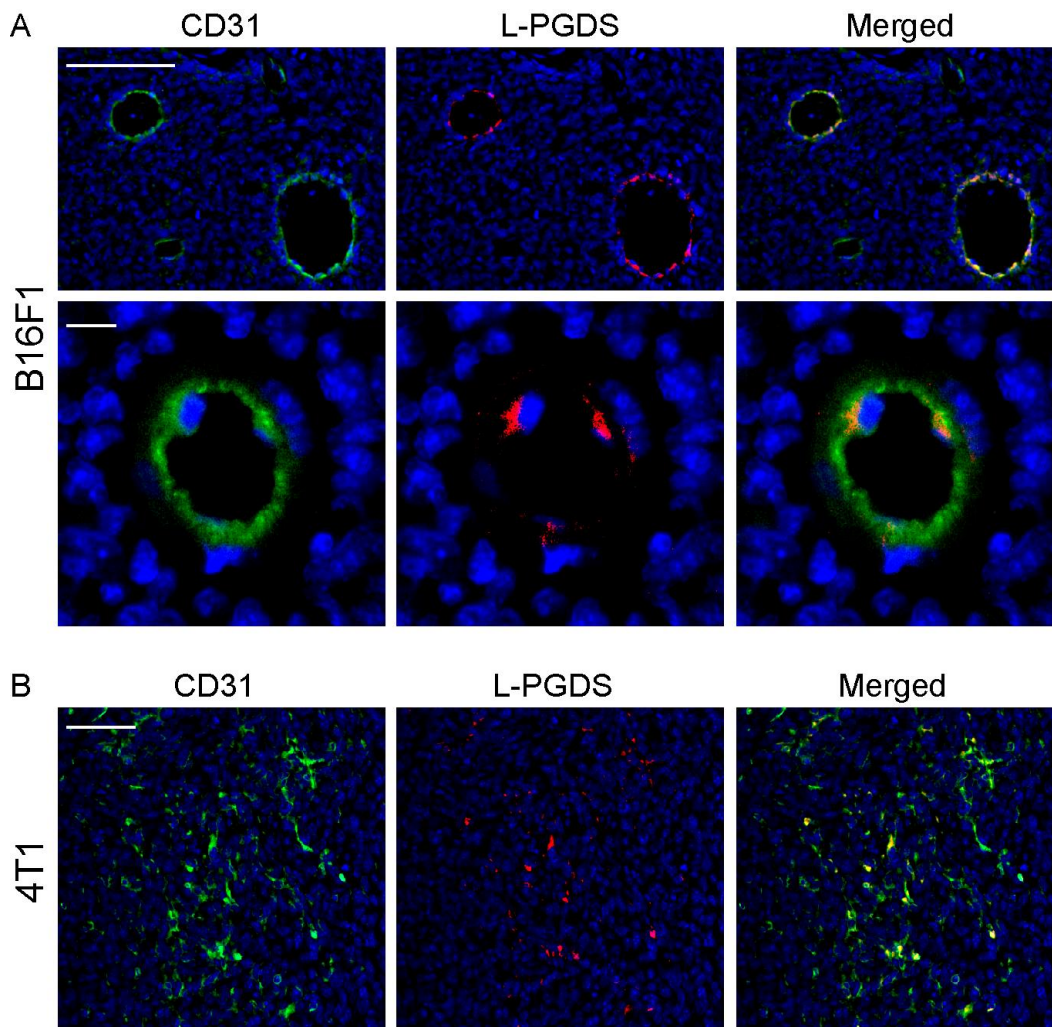


**Figure 5 L-PGDS was localized in B16F1 melanoma and 4T1 ECs**

(A) Representative pictures of tumor immunostaining of CD31 (green), L-PGDS (red), and DAPI (blue) in B16F1 melanoma. Scale bar, 100  $\mu\text{m}$  (upper panels) and 10  $\mu\text{m}$  (lower panels). (B) Representative pictures of tumor immunostaining of CD31 (green), L-PGDS (red), and DAPI (blue) in 4T1. Scale bar, 100  $\mu\text{m}$ .

#### 2-2-4 Localization of L-PGDS in human tumor

In addition to ECs in mice tumor, *In situ* hybridization showed mRNA expression of L-PGDS in ECs in human melanoma and oral squamous cell carcinoma tissues (Fig. 6, white arrow heads). Its expression was also detected in some melanoma cells (Fig. 6, black arrow-heads).

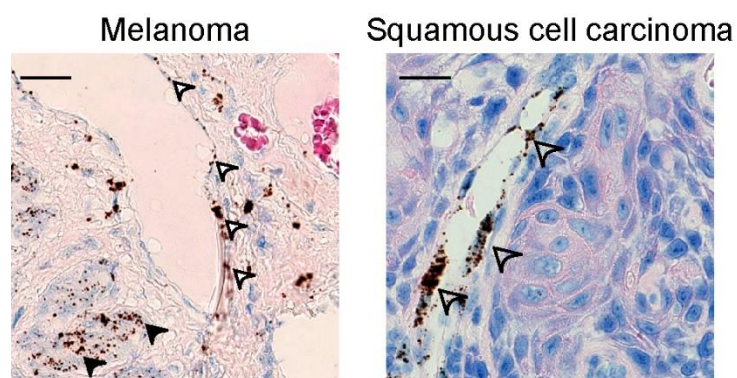


**Figure 6 L-PGDS was expressed in ECs of human tumors**

Representative pictures of L-PGDS *in situ* hybridization in human melanoma (left) and oral squamous cell carcinoma (right). White arrow heads indicate positive staining of L-PGDS in ECs, and black arrow heads indicate positive staining of L-PGDS in tumor cells. Scale bar, 25  $\mu$ m.

### 2-2-5 Expression of L-PGDS in melanoma supernatant-treated EC

ECs in tumor are considered to have acquired their abnormal characteristics due to sustained inflammatory stimuli, including tumor cell-derived cytokines and growth factors in the tumor microenvironment (4). I determined the effect of tumor cell-derived factors on mRNA expression of L-PGDS in normal ECs (HUVECs) by treating supernatant from melanoma cell culture. As shown in Fig. 7, 3 h or 6 h stimulation to a minor extent, and 12 h stimulation markedly, increased the expression of L-PGDS. This increase in levels of L-PGDS persisted for at least 24 h.

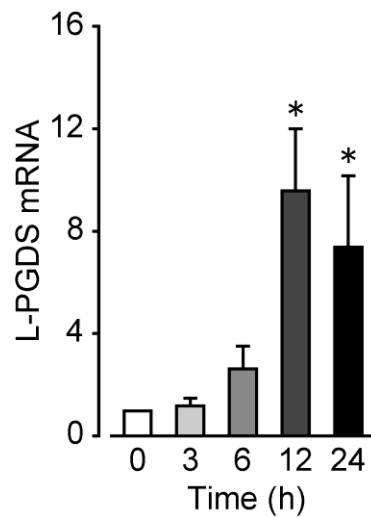


**Figure 7 L-PGDS was upregulated by melanoma supernatant in EC**

The time-dependent effect of melanoma culture supernatant on the mRNA expression of L-PGDS in HUVECs (n = 5). \* Significantly different from the results in none treated cells at  $p < 0.05$ . Data are presented as means  $\pm$  SEM.

### 2-2-6 Effect of IL-1 or TNF- $\alpha$ antagonist on expression of L-PGDS in EC

I next evaluated which factors in culture supernatant stimulate the expression of L-PGDS. As shown in Fig. 8, pretreatment with IL-1 receptor antagonist, IL-1Ra (500 ng/ml, 1 h) or TNF- $\alpha$  receptor antagonist, WP9QY (25  $\mu$ M, 1 h) significantly inhibited the elevation of L-PGDS levels. Co-treatment with these antagonists inhibited L-PGDS upregulation by about 80% (Fig. 8).

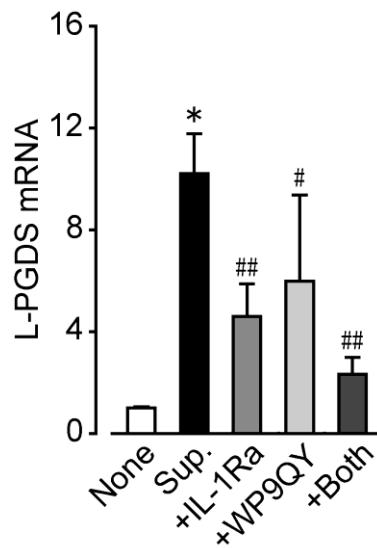


**Figure 8 IL-1 and TNF- $\alpha$  inhibition attenuated L-PGDS upregulation in EC**

The effect of IL-1 antagonist (IL-1Ra, n = 6), TNF- $\alpha$  antagonist (WP9QY, n = 5), or IL-1Ra and WP9QY (n = 6) on the mRNA expression of L-PGDS in melanoma supernatant-treated (n = 8) HUVECs. \* Significantly different from the results in none treated cells at  $p < 0.05$ . ## Significantly different from culture supernatant treated cells at  $p < 0.05$  or  $p < 0.01$ , respectively. Data are presented as means  $\pm$  SEM.

### 2-2-7 Effect of tyrosine kinase or COX inhibitor on expression of L-PGDS in EC

In contrast the results in Fig. 8, pretreatment with a pan-tyrosine kinase inhibitor, genistein (Gen, 100  $\mu$ M, 1 h) or a COX inhibitor, indomethacin (Indo, 20  $\mu$ M, 1 h) did not alter the mRNA expression of L-PGDS (Fig. 9), indicating that these signaling did not affect L-PGDS upregulation in HUVECs.

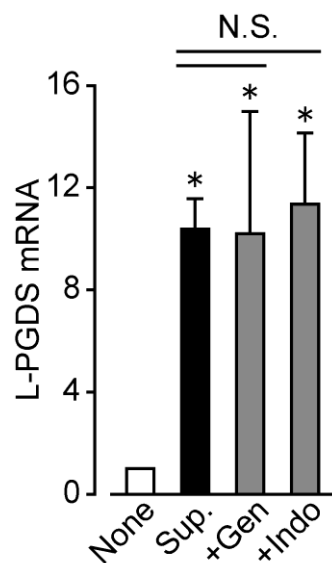


**Figure 9 Tyrosine kinase or COX inhibition did not alter mRNA expression of L-PGDS in EC**

The effect of tyrosine kinase inhibitor (Genistein; Gen) or COX inhibitor (Indomethacin; Indo) on mRNA expression of L-PGDS in melanoma supernatant-treated HUVECs (n = 6). \* Significantly different from the results in none treated cells at  $p < 0.05$ .

<sup>N.S.</sup> No significance. Data are presented as means  $\pm$  SEM.

### **2-2-8 PGD<sub>2</sub> production in melanoma supernatant-treated EC**

Consistent with the results in mRNA expression of L-PGDS, the production of PGD<sub>2</sub> was also increased in HUVECs treated with melanoma culture supernatant (Fig. 10). Its production was inhibited by pretreatment with a L-PGDS inhibitor, AT-56 (100-300 μM, 1 h). Co-pretreatment with IL-1Ra and WP9QY almost completely inhibited the production of PGD<sub>2</sub> (Fig. 10). Pretreatment with an inhibitor of another PGD<sub>2</sub> synthase, hematopoietic-PGDS (H-PGDS), HQL-79 (1-10 μM, 1 h), had little effect on the PGD<sub>2</sub> production.

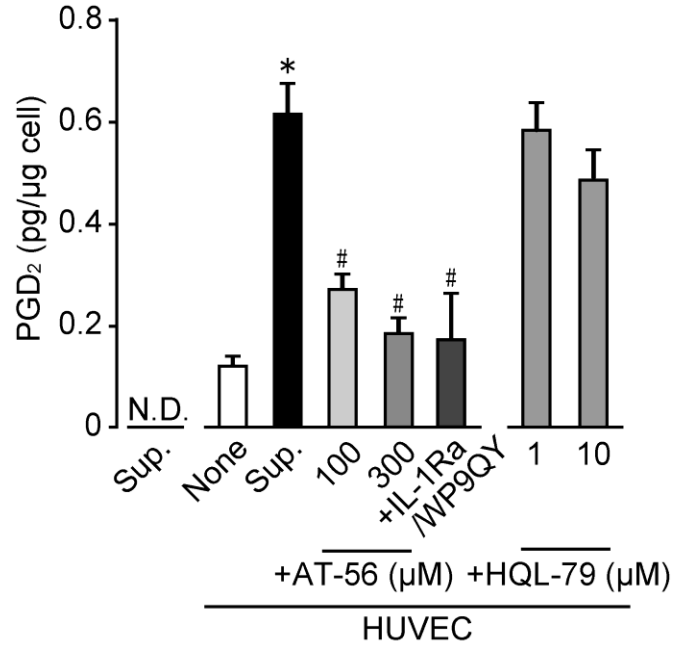


**Figure 10 IL-1 and TNF- $\alpha$  inhibition attenuated PGD<sub>2</sub> production in EC**

The effect of L-PGDS inhibitor (AT-56), IL-1 antagonist (IL-1Ra) and TNF- $\alpha$  antagonist (WP9QY) (n = 6), or H-PGDS inhibitor (HQL-79, n = 6) on melanoma supernatant-treated (n = 10) PGD<sub>2</sub> production in HUVECs. \* Significantly different from the results in none treated cells at p < 0.05. # Significantly different from culture supernatant treated cells at p < 0.05 or p < 0.01, respectively. Data are presented as means  $\pm$  SEM.

## 2-3 Role of endothelial L-PGDS in tumor growth

### 2-3-1 Melanoma or LLC growth in WT and L-PGDS deficient mice

I next evaluated the role of L-PGDS in tumor growth by using L-PGDS deficient (L-PGDS<sup>-/-</sup>) mice. As shown in Fig. 11A, melanoma cells implanted in mice flanks grew faster in L-PGDS<sup>-/-</sup> mice compared to WT mice. The tumor size doubled in 16 days after the implantation. L-PGDS<sup>-/-</sup> mice also exhibited rapid tumor growth in LLC (Fig. 11B).

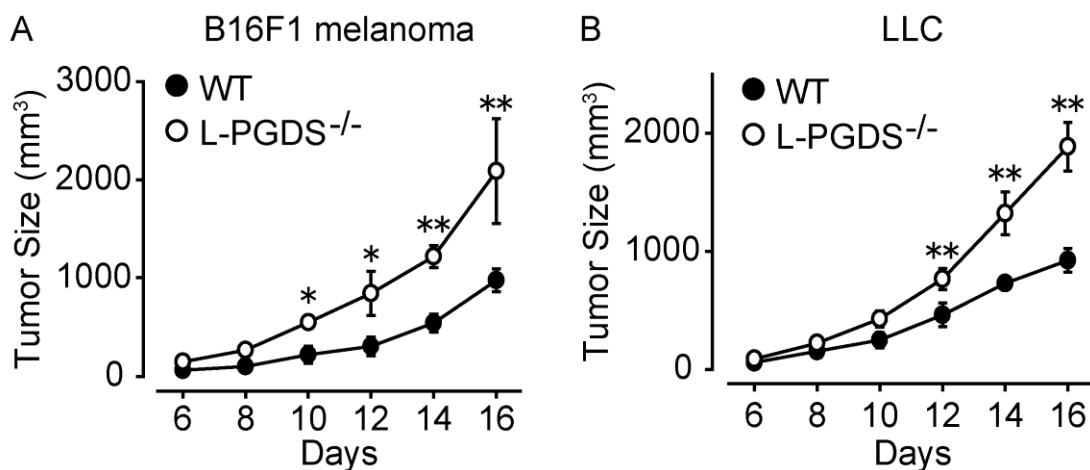


**Figure 11 Systemic L-PGDS deficiency exacerbated tumor growth**

(A) Growth rate of melanoma growth in WT and L-PGDS<sup>-/-</sup> mice (n = 6). (B) Growth rate of LLC in WT and L-PGDS<sup>-/-</sup> mice (n = 5-6). \*\* Significantly different from the results in WT mice at p < 0.01. Data are presented as means ± SEM.

### 2-3-2 PGD<sub>2</sub> content in WT and L-PGDS<sup>-/-</sup> mice tumor

I next measured the PGD<sub>2</sub> content in tumor. About 5 pg/mg tissue of PGD<sub>2</sub> was detected in melanoma grown in WT mice (Fig. 12). Host deficiency of the L-PGDS gene significantly decreased the PGD<sub>2</sub> content in melanoma by 60% (Fig. 12).

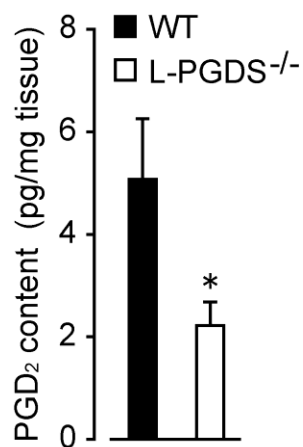


**Figure 12** Decrease of PGD<sub>2</sub> content in tumor of L-PGDS<sup>-/-</sup> mice

PGD<sub>2</sub> content in WT and L-PGDS<sup>-/-</sup> mice tumor (n = 19). \* Significantly different from the results in WT mice at p < 0.05. Data are presented as means ± SEM.

### 2-3-3 Effect of DP agonist on tumor growth

The biological actions of  $\text{PGD}_2$  are mediated through two G protein-coupled receptors, DP and CRTH2. Previous report showed that DP was localized in tumor ECs (38). As shown below, treatment with a DP receptor agonist, BW245C (BW, 0.1 mg/kg, intraperitoneal, twice a day) significantly inhibited tumor growth both in WT and L-PGDS<sup>-/-</sup> mice (Fig. 13), indicating that  $\text{PGD}_2$  inhibited tumor growth through DP.

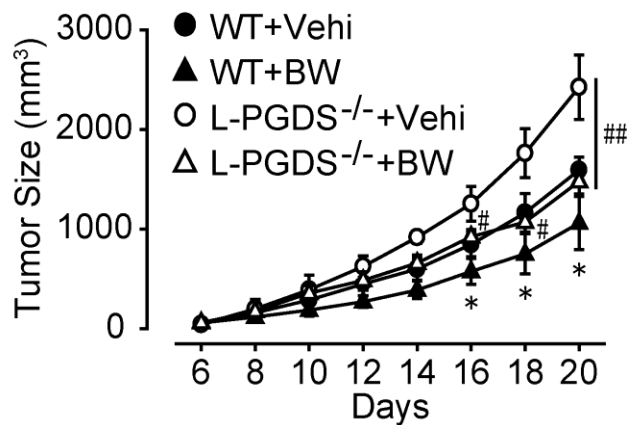


**Figure 13 Treatment with DP agonist inhibited tumor growth in WT and L-PGDS<sup>-/-</sup> mice**

The effect of DP agonist, BW245C (BW), in WT and L-PGDS<sup>-/-</sup> mice tumor growth (n = 6). \* Significantly different from the results in WT+Vehi at p < 0.05. #,## Significantly different from the results in L-PGDS<sup>-/-</sup> Vehi mice at p < 0.05 or p < 0.01, respectively. Data are presented as means  $\pm$  SEM.

### 2-3-4 Tumor growth in CRTH2 deficient mice

I also evaluated the role of CRTH2 in tumor growth. Host gene deficiency of CRTH2 did not influence the growth of B16F1 melanoma on WT mice (Fig. 14).

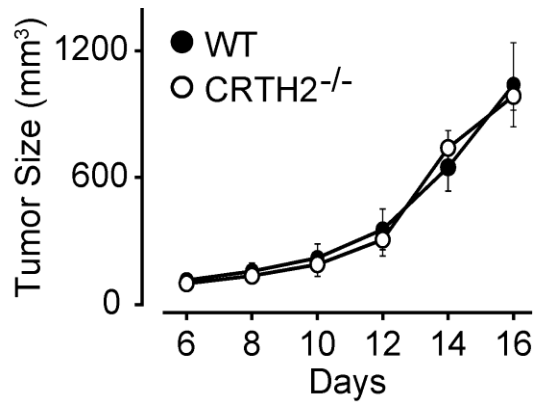


**Figure 14 CRTH2 deficiency did not alter tumor growth**

Growth rate of melanoma in WT and CRTH2 deficient (CRTH2<sup>-/-</sup>) mice (n = 4).

Data are presented as means ± SEM.

### 2-3-5 Effect of PGD<sub>2</sub> on cultured tumor cell proliferation and survival

I also confirmed that PGD<sub>2</sub> (0.1-10  $\mu$ M, 6-24 h) had no direct effect on proliferation and survival of melanoma *in vitro* (Fig. 15). These data suggested that PGD<sub>2</sub> attenuated tumor growth by modulating the tumor microenvironment.

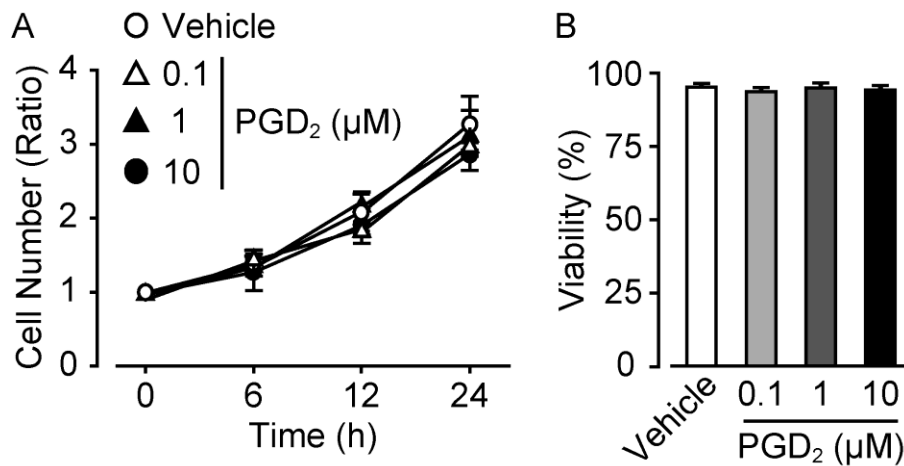


**Figure 15 PGD<sub>2</sub> did not affect tumor proliferation and survival *in vitro***

The effect of PGD<sub>2</sub> (0.1-10  $\mu$ M) on proliferation (6-24 h) or viability (24 h) of B16F1 melanoma cell (n = 5). Data are presented as means  $\pm$  SEM.

### 2-3-6 Tumor growth in WT or L-PGDS<sup>-/-</sup> bone marrow transplanted mice

I attempted to find the functional source of PGD<sub>2</sub> in growing tumors using bone marrow transplantation. L-PGDS<sup>-/-</sup> bone marrow-implanted WT mice (WT + L-PGDS<sup>-/-</sup>BM) showed equivalent tumor growth compared to WT mice (Fig. 16). In contrast, WT bone marrow-implanted L-PGDS<sup>-/-</sup> mice (L-PGDS<sup>-/-</sup> + WT<sup>BM</sup>) showed accelerated tumor growth which was comparable to that of L-PGDS<sup>-/-</sup> mice (Fig. 16). These results indicated that the non-myeloid cell-derived L-PGDS was responsible for the inhibition of tumor growth.

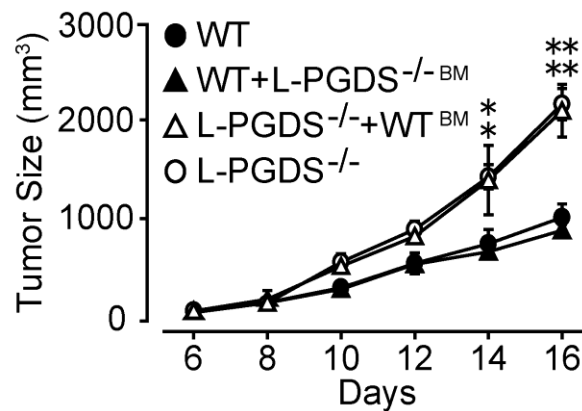


**Figure 16 L-PGDS deficiency in non-myeloid cells exacerbated tumor growth**

Growth rate of melanoma in bone marrow transplanted mice (n = 5). \*,\*\* Significantly different from the results in WT mice at p < 0.05 or p < 0.01, respectively. Data are presented as means ± SEM.

### 2-3-7 Tumor growth in endothelial-specific L-PGDS deficient mice

I further assessed tumor growth in endothelial specific L-PGDS deficient (L-PGDS<sup>ΔEC</sup>) mice. As shown in Fig. 17, implanted melanoma grew faster in L-PGDS<sup>ΔEC</sup> mice compared to that in control (L-PGDS<sup>fl/fl</sup>) mice. These observations suggested that the L-PGDS-PGD<sub>2</sub>-DP signaling pathway in ECs inhibited tumor growth.

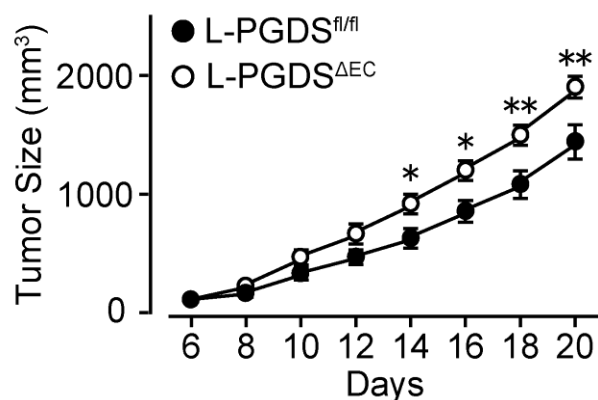


**Figure 17 L-PGDS deficiency in endothelial cells exacerbated tumor growth**

Growth rate of melanoma in L-PGDS<sup>fl/fl</sup> (n = 8) or L-PGDS<sup>ΔEC</sup> mice (n = 9). \*\*\*\* Significantly different from the results in L-PGDS<sup>fl/fl</sup> mice at p < 0.05 or p < 0.01, respectively. Data are presented as means ± SEM.

## **2-4 Morphological analysis of tumor**

### **2-4-1 HE staining of tumor**

Tumor growth is the net result of tumor cell proliferation and death. HE-stained tumor sections from WT mice showed a necrotic layer spread throughout the tumor (Fig. 18A, black arrow heads). L-PGDS deficiency in the host significantly decreased the necrotic area in the tumor (Fig. 18A, B). Similar results were also obtained from L-PGDS<sup>ΔEC</sup> mice (Fig. 18C, D)

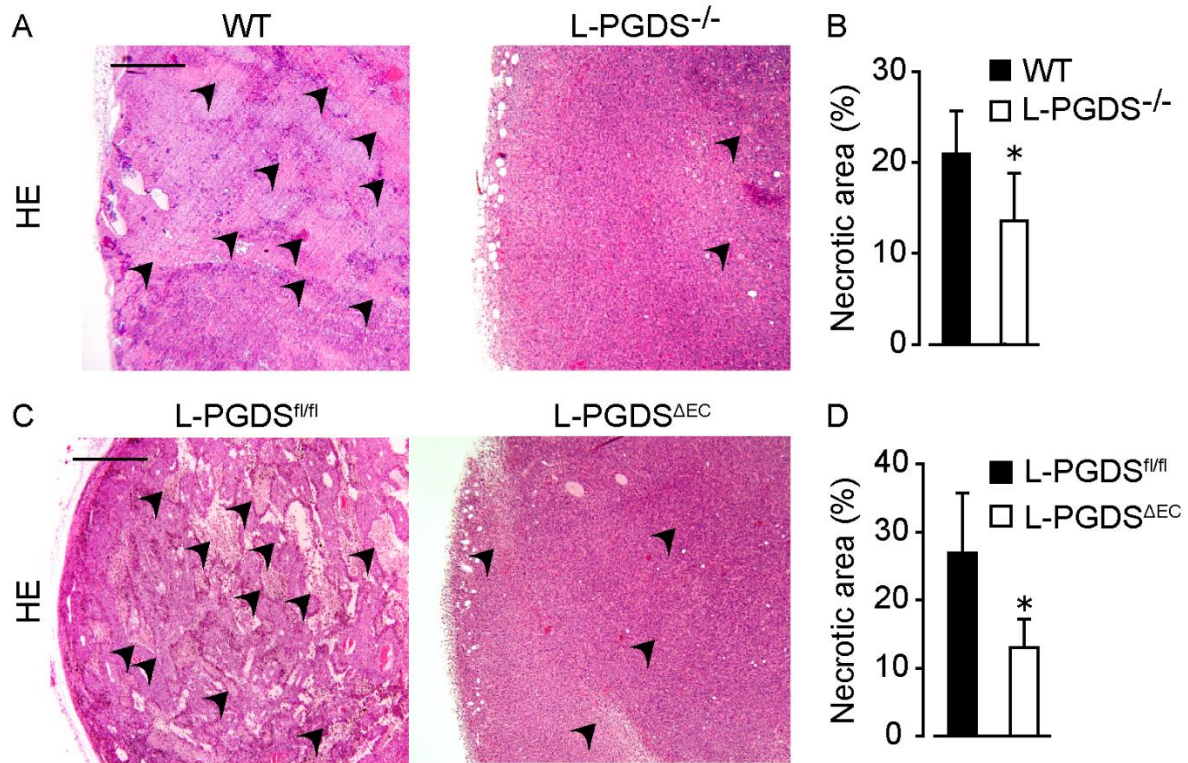


**Figure 18 Endothelial L-PGDS deficiency decreased necrotic area in the tumor**

(A) Representative pictures of HE staining in melanoma. Arrow heads indicate necrotic layer in tumor. Scale bar, 200  $\mu$ m. (B) Quantification of necrotic layer in tumor (n = 5). (C) Representative pictures of HE staining in melanoma. Arrow heads indicate necrotic layer in tumor. Scale bar, 200  $\mu$ m. (D) Quantification of necrotic layer in tumor (n = 6). \* Significantly different from the results in WT or L-PGDS<sup>fl/fl</sup> mice at  $p < 0.05$ . Data are presented as means  $\pm$  SEM.

#### 2-4-2 Proliferative rate of tumor

I examined the proliferation of tumor in WT, L-PGDS<sup>-/-</sup>, and L-PGDS<sup>ΔEC</sup> mice. The number of Ki67 positive proliferative tumor cells was not different between the tumors in the WT and L-PGDS<sup>-/-</sup> mice (Fig. 19A, B) and also between the tumors in L-PGDS<sup>fl/fl</sup> and L-PGDS<sup>ΔEC</sup> mice (Fig. 19C, D).

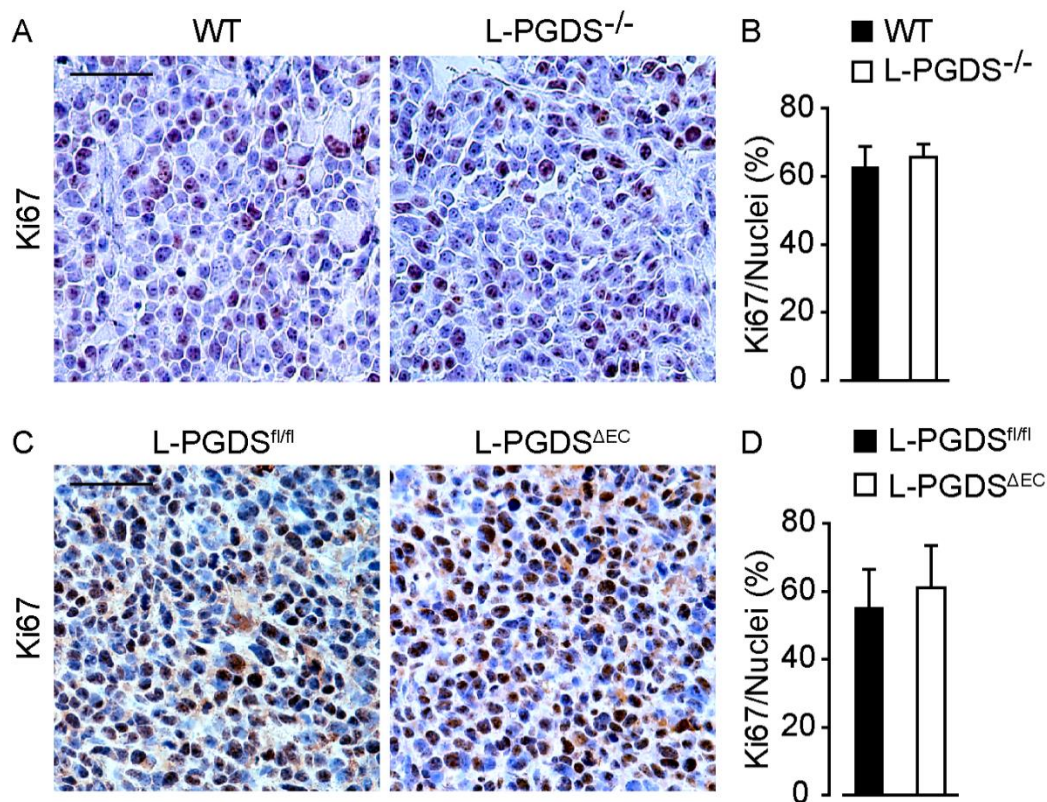


**Figure 19 L-PGDS deficiency did not alter the number of proliferative cells in tumor**

(A) Representative pictures of Ki67 staining in melanoma. Scale bar, 50 μm. (B) Quantification of Ki67 positive cells in tumor (n = 5). (C) Representative pictures of Ki67 staining in melanoma. Scale bar, 50 μm. (D) Quantification of Ki67 positive cells in tumor (n = 6). Data are presented as means ± SEM.

### **2-4-3 Apoptotic rate of tumor**

I also examined the number of TUNEL positive apoptotic cells and found significant reduction in the tumors in L-PGDS<sup>-/-</sup> mice (Fig. 20A, B), suggesting that host L-PGDS deficiency increased tumor growth by attenuating tumor cell death. I also confirmed the similar observations in L-PGDS<sup>ΔEC</sup> mice (Fig. 20C, D).

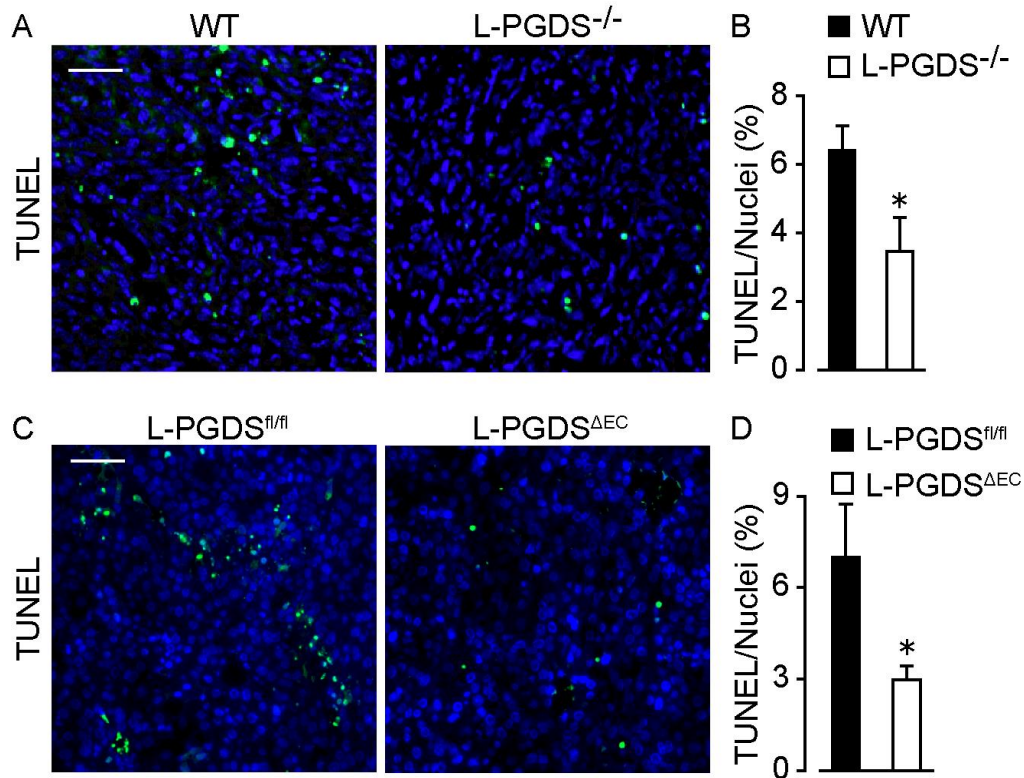


**Figure 20 Endothelial L-PGDS deficiency decreased the number of apoptotic cells in tumor**

(A) Representative pictures of TUNEL staining in melanoma. Scale bar, 50  $\mu$ m. (B) Quantification of TUNEL positive cells in tumor (n = 5). (C) Representative pictures of TUNEL staining in melanoma. Scale bar, 50  $\mu$ m. (D) Quantification of TUNEL positive cells in tumor (n = 5). \* Significantly different from the results in WT or L-PGDS<sup>fl/fl</sup> mice at  $p < 0.05$ . Data are presented as means  $\pm$  SEM.

## **2-5 Role of endothelial L-PGDS in tumor vessels**

### **2-5-1 Hypoxic region in tumor**

I hypothesized that L-PGDS-PGD<sub>2</sub> increased the number of apoptotic tumor cells by limiting nutrient/oxygen delivery. The tumor implanted WT mice exhibited hypoxic area throughout the tumor mass (Fig. 21A upper left panel). The area was markedly decreased in L-PGDS<sup>-/-</sup> mice tumor (Fig. 21A lower left panel and Fig. 22B), suggesting the efficient delivery of oxygen.

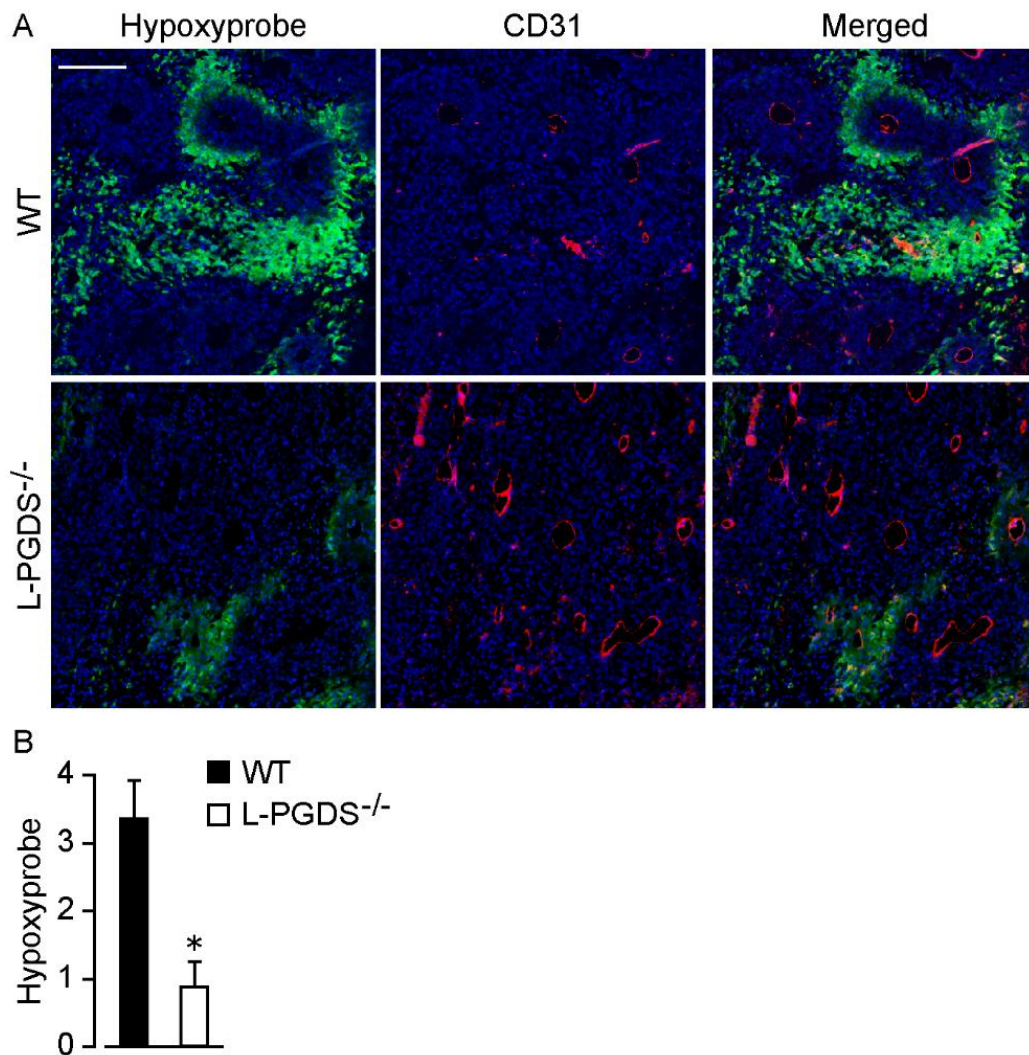


**Figure 21 L-PGDS deficiency decreased hypoxic area in tumor**

(A) Representative pictures of tumor immunostaining of DAPI (blue), Hypoxyprobe (green), and CD31 (red) in WT and L-PGDS<sup>-/-</sup> mice. Scale bar, 100  $\mu$ m. (B) Quantification of Hypoxyprobe intensity (n = 5). \* Significantly different from the results in WT mice at p < 0.05. Data are presented as means  $\pm$  SEM.

### **2-5-2 Angiogenesis and vascular permeability in tumor**

Since L-PGDS was specifically localized in tumor ECs, I next focused on tumor vascular function. WT mice tumor exhibited neovascularization (Fig. 22A upper left panel) and vascular leakage (fibrinogen deposition outside the vessels, Fig. 22A upper middle panel). Tumor sections from L-PGDS<sup>-/-</sup> and L-PGDS<sup>ΔEC</sup> mice revealed increase in tumor angiogenesis (indicated as the number of CD31 positive tumor ECs; Fig. 22A lower left panel, Fig. 22B, Fig. 22C lower left panel, and Fig. 22D) and vascular leakage (indicated as the amount of fibrinogen deposition; Fig. 22A lower middle panel, Fig. 22B, Fig. 22C lower middle panel, and Fig. 22D).

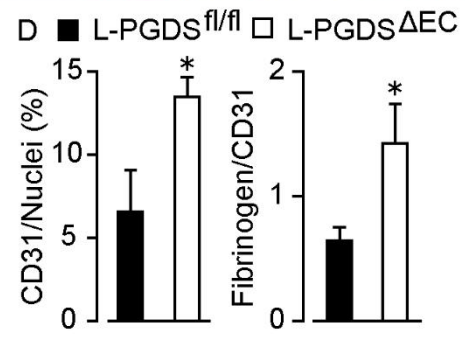
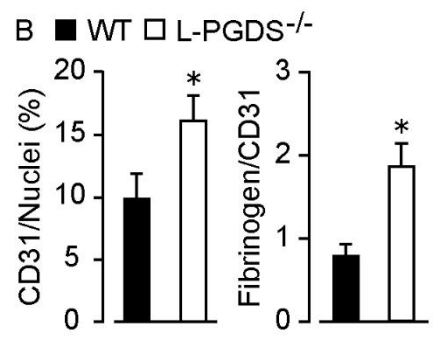
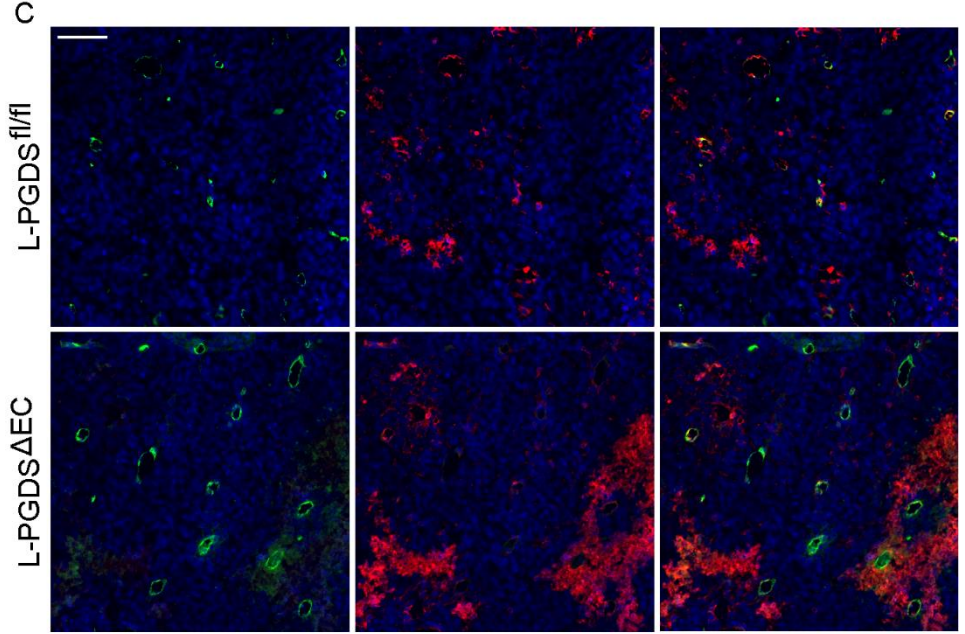
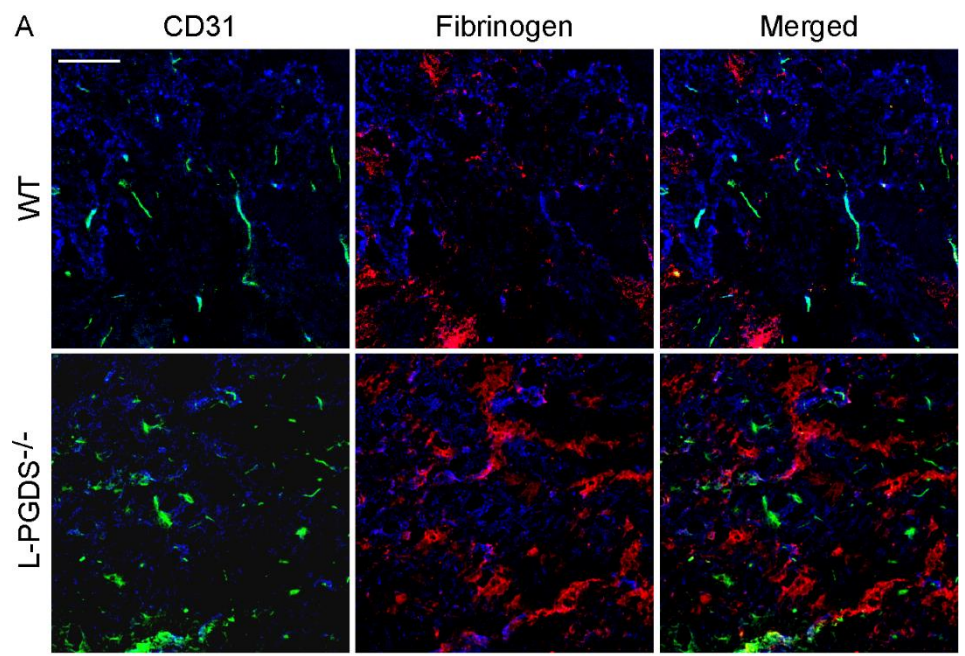
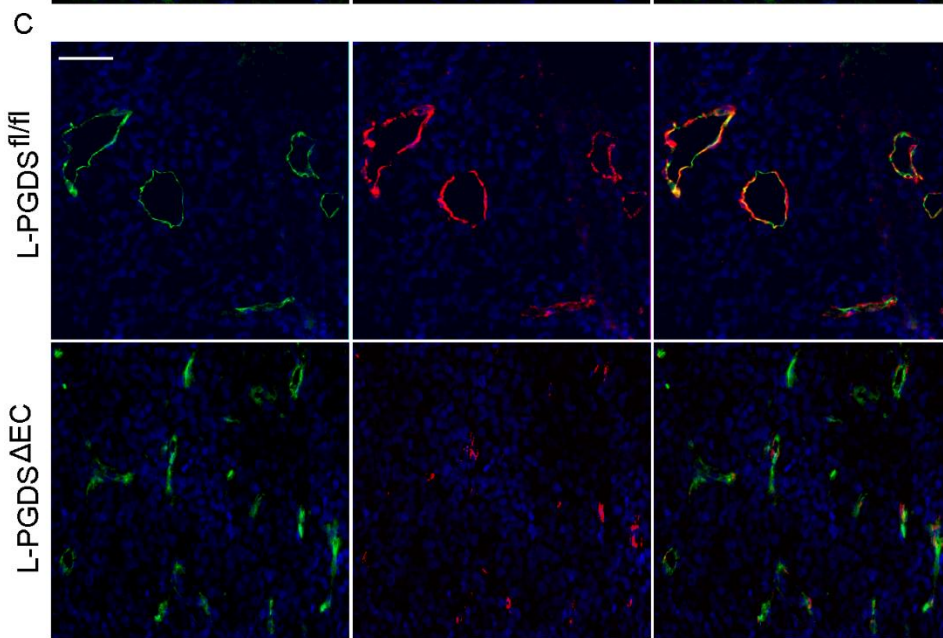
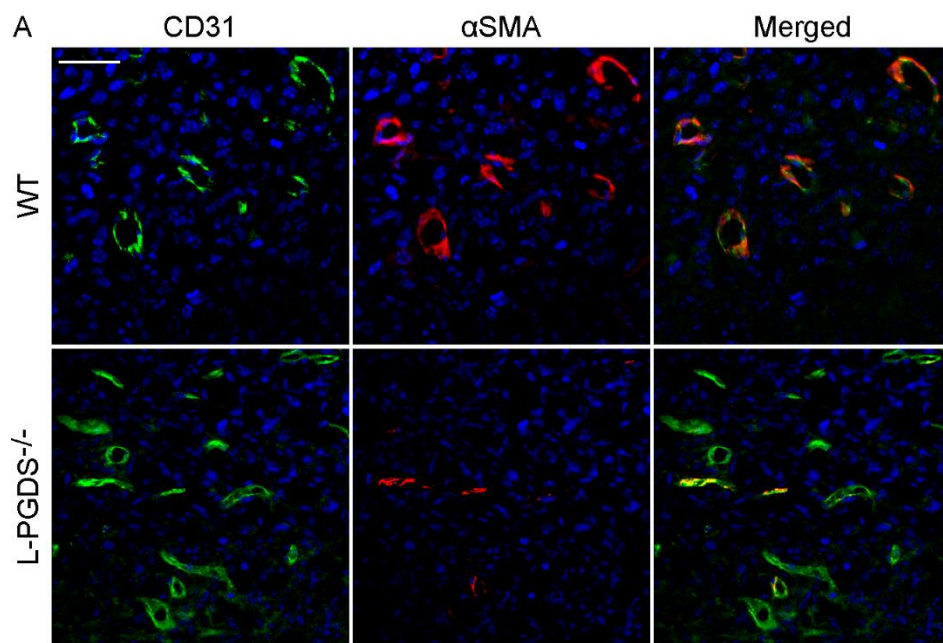


**Figure 22 Endothelial L-PGDS deficiency enhanced tumor angiogenesis and vascular permeability**

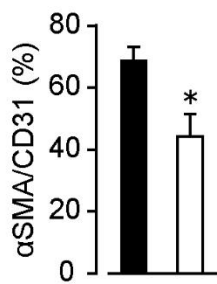
(A) Representative pictures of tumor immunostaining of DAPI (blue), CD31 (green), and fibrinogen (red). Scale bar, 100  $\mu\text{m}$ . (B) Quantification of CD31 positive cells (to the ratio of total cells,  $n = 5$ ) and fibrinogen intensity (to the ratio of CD31 intensity,  $n = 5$ ). (C) Representative pictures of tumor immunostaining of DAPI (blue), CD31 (green), and fibrinogen (red). Scale bar, 100  $\mu\text{m}$ . (D) Quantification of CD31 positive cells ( $n = 6$ ) and fibrinogen intensity (to the ratio of CD31 intensity,  $n = 6$ ). \* Significantly different from the results in WT or L-PGDS<sup>fl/fl</sup> mice at  $p < 0.05$ . Data are presented as means  $\pm$  SEM.

### **2-5-3 Vessel maturation in tumor**

In addition to increase in vascular angiogenesis and permeability, the CD31 positive tumor ECs in the L-PGDS<sup>-/-</sup> and L-PGDS<sup>ΔEC</sup> mice exhibited less αSMA positive smooth muscle coverage ratio (about 40-50% of CD31<sup>+</sup> tumor ECs were covered) compared to the respective control (about 60-70% of CD31<sup>+</sup> tumor ECs were covered) (Fig. 23A middle panels, Fig. 23B, Fig. 23C middle panels, and Fig. 23D), indicating less mature vasculature.



**B** ■ WT □ L-PGDS<sup>-/-</sup>



**D** ■ L-PGDS<sup>fl/fl</sup> □ L-PGDS $\Delta$ EC

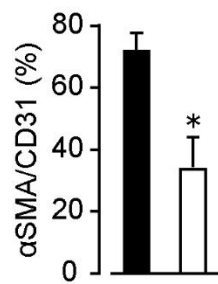


**Figure 23 Endothelial L-PGDS deficiency decreased the number of  $\alpha$ SMA-covered mature vessels**

(A) Representative pictures of tumor immunostaining of DAPI (blue), CD31 (green), and  $\alpha$ SMA (red). Scale bar, 50  $\mu$ m. (B) Quantification of  $\alpha$ SMA positive cells (to the ratio of CD31 positive cells) in tumor (n = 5). (C) Representative pictures of tumor immunostaining of DAPI (blue), CD31 (green), and  $\alpha$ SMA (red). Scale bar, 50  $\mu$ m. (D) Quantification of  $\alpha$ SMA positive cells (to the ratio of CD31 positive cells) in tumor (n = 6).

\* Significantly different from the results in WT or L-PGDS<sup>fl/fl</sup> mice at p < 0.05. Data are presented as means  $\pm$  SEM.

#### **2-5-4 Functional vessels in tumor**

Most tumor vessels are disrupted and hardly perfused, thus limiting their ability to deliver enough oxygen and nutrients. I also examined vessel perfusion in the tumor. About 10% of CD31 positive ECs composed lectin positive perfused vessels (Fig. 24A upper panels and Fig. 24B). The ratio of perfused vessels was doubled in L-PGDS<sup>-/-</sup> mice (Fig. 24A lower panels and Fig. 24B), indicating the increase of function vessels. These observations suggested that L-PGDS-PGD<sub>2</sub> signaling reduced vascular leakage, angiogenesis, and perfusion, thereby leading to decrease tumor growth.

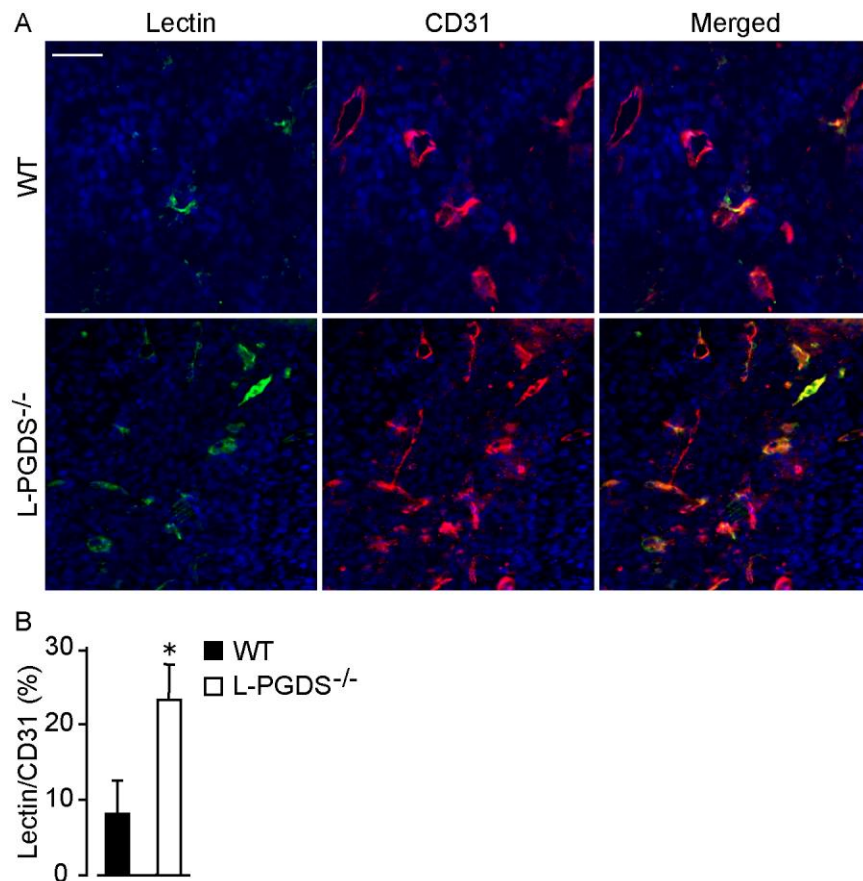
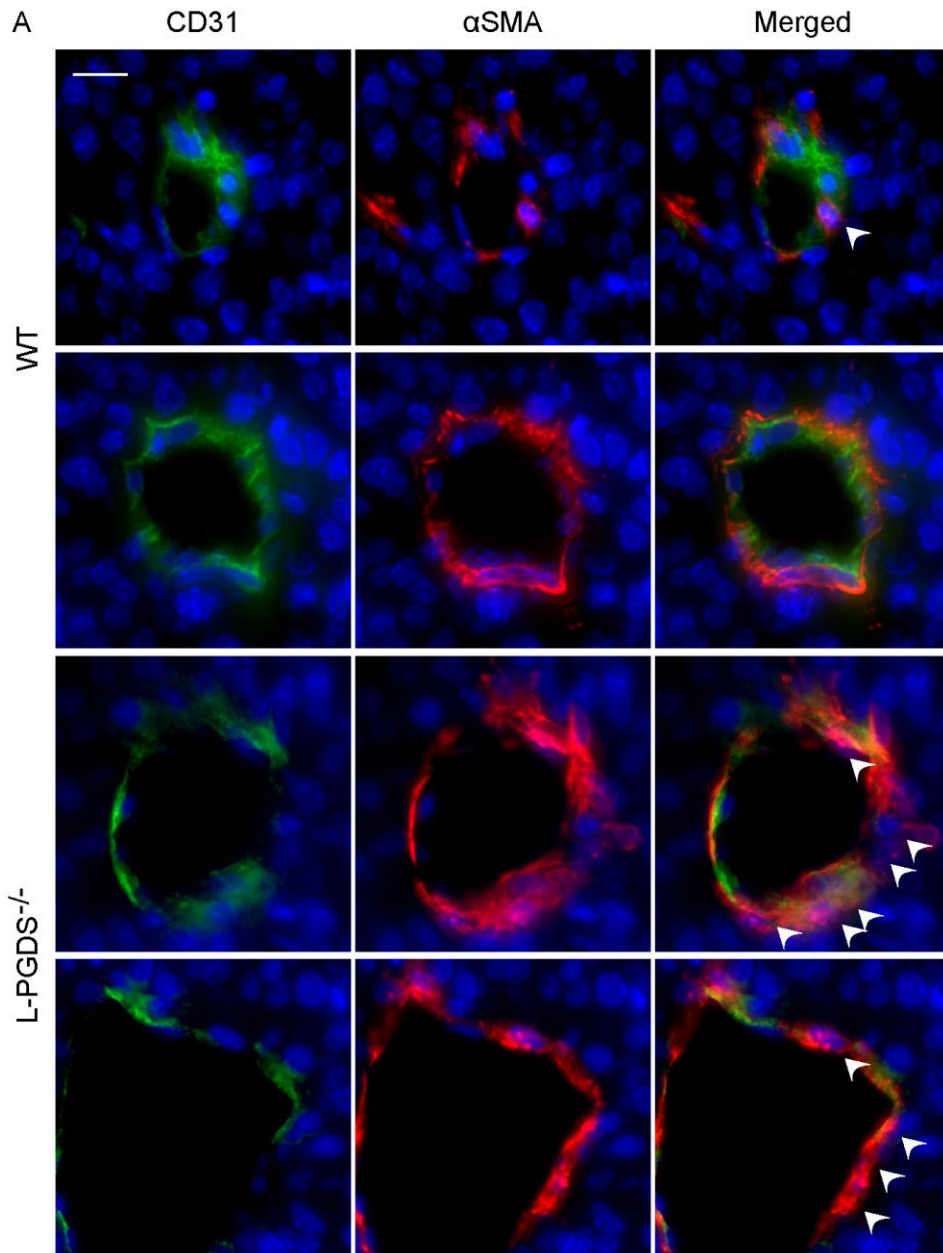


**Figure 24 L-PGDS deficiency increased the number of functional vessels in tumor**

(A) Representative pictures of tumor immunostaining of DAPI (blue), Lectin (green) and CD31 (red). Scale bar, 50  $\mu$ m. (B) Quantification of Lectin positive cells (to the ratio of CD31 positive cells) in tumor (n = 5). \* Significantly different from the results in WT mice at  $p < 0.05$ . Data are presented as means  $\pm$  SEM.

### **2-5-5 Endothelial-to-mesenchymal transition in tumor**

I next speculated that endothelial L-PGDS-PGD<sub>2</sub> autocrine loop might induce phenotypic changes of tumor ECs, known as Endothelial-to-mesenchymal transition (EndMT). In WT mice, about 6% of CD31 positive tumor ECs were also positive for EndMT marker,  $\alpha$ SMA (Fig. 25A white arrow head, and Fig. 25B), indicating the phenotypic conversion of ECs to mesenchymal cells. The ratio of the CD31/ $\alpha$ SMA double positive cells was increased about 50% in L-PGDS<sup>-/-</sup> mice (Fig. 25A white arrow head and Fig. 25B).



**B** ■ WT □ L-PGDS<sup>-/-</sup>

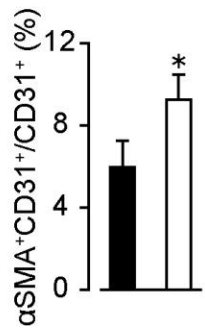


**Figure 25 L-PGDS deficiency enhanced EndMT in tumor**

(A) Representative pictures of tumor immunostaining of DAPI (blue), CD31 (green), and  $\alpha$ SMA (red). Arrow heads indicate CD31/ $\alpha$ SMA double positive, EndMT occurred cells. Scale bar, 15  $\mu$ m. (B) Quantification of  $\alpha$ SMA and CD31 double positive cells (to the ratio of CD31 positive cells) in tumor (n = 8). \* Significantly different from the results in WT mice at  $p < 0.05$ . Data are presented as means  $\pm$  SEM.

## 2-5-6 mRNA expression of EndMT markers in tumor ECs

I also examined the role of L-PGDS in EndMT using tumor ECs isolated from melanoma. L-PGDS deficiency markedly increased the mRNA expression of  $\alpha$ SMA compared to that of WT ECs (Fig. 26, middle graph), while it did not influence the mRNA expression of Cdh5 (endothelial marker; also known as VE-cadherin, left graph) and transforming growth factor  $\beta$  (TGF $\beta$ , main EndMT induction molecule, right graph).

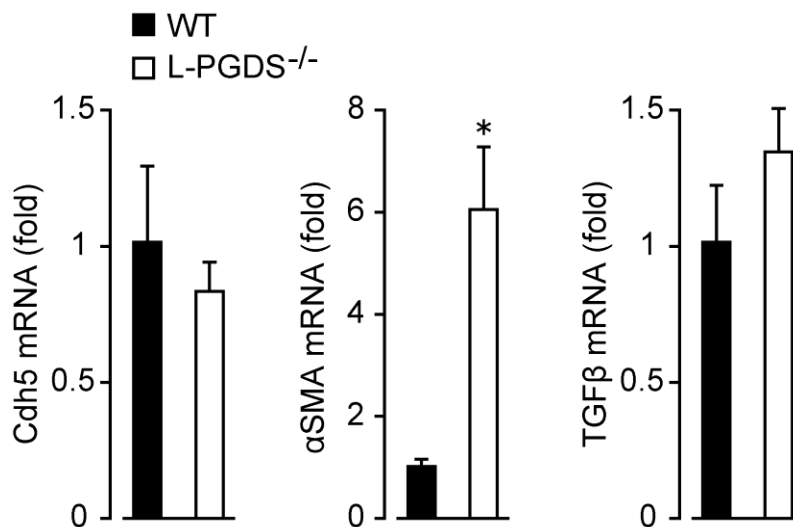


**Figure 26 L-PGDS deficiency increased the mRNA expression of EndMT marker in tumor ECs**

mRNA expression of Cdh5,  $\alpha$ SMA, and TGF $\beta$  in isolated ECs (n = 6). \* Significantly different from the results in WT ECs at p < 0.05. Data are presented as means  $\pm$  SEM.

### 2-5-7 mRNA expression of EndMT markers in melanoma supernatant-treated EC

I finally evaluated the role of L-PGDS in EndMT using isolated human ECs. Inhibition of L-PGDS (AT-56, 100  $\mu$ M, 1 h) significantly increased the mRNA expression of  $\alpha$ SMA in melanoma supernatant (12 h)-treated HUVECs, suggesting that L-PGDS inhibition facilitated EndMT *in vitro* (Fig. 27). Taken together, endothelial L-PGDS also attenuated the malignant properties of tumor by inhibiting the transformation of ECs to mesenchymal cells.

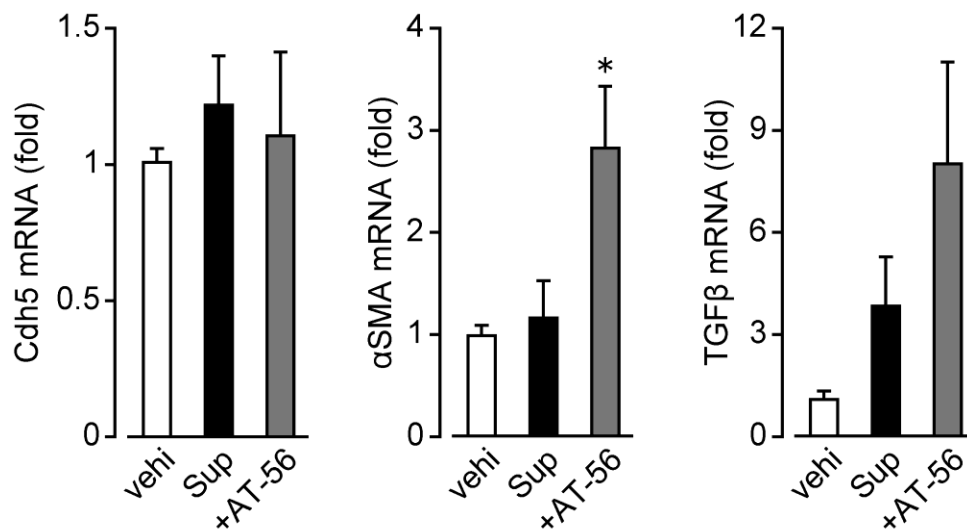


**Figure 27 L-PGDS inhibition increased mRNA expression of EndMT marker in EC**

mRNA expression of Cdh5,  $\alpha$ SMA, and TGF $\beta$  in melanoma culture supernatant-treated HUVECs (n = 5). \* Significantly different from the results in supernatant-treated HUVECs at p < 0.05. Data are presented as means  $\pm$  SEM.

### **2-5-8 Immune cell infiltration in tumor**

I examined the difference in immune cell infiltration between WT and L-PGDS<sup>-/-</sup> mice tumor. In contrast to effects on vessel morphology and function mentioned above, L-PGDS deficiency did not influence the infiltration of inflammatory cells such as CD68<sup>+</sup> monocytes/macrophages, Gr-1<sup>+</sup> granulocytes, and CD4<sup>+</sup> T cells in tumor (Fig. 28).

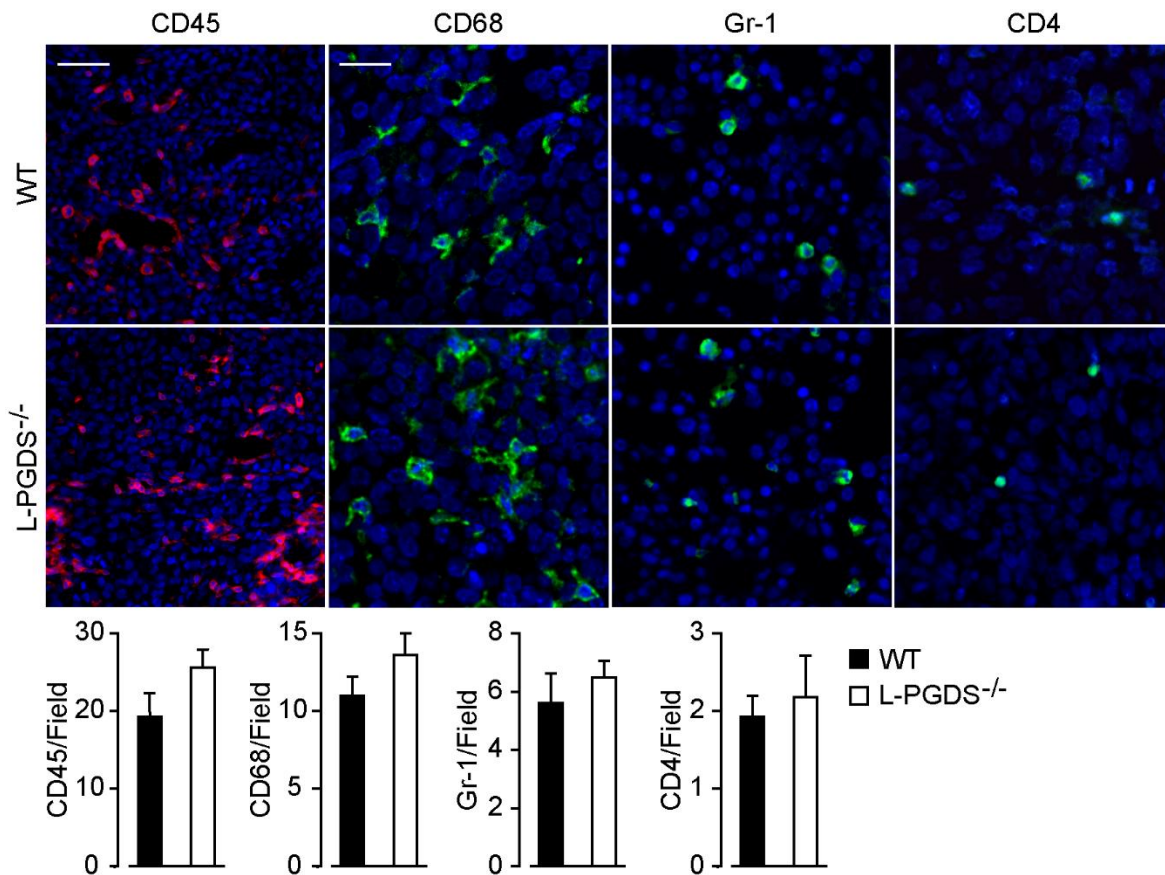


**Figure 28 L-PGDS deficiency did not alter the number of immune cell infiltration in tumor**

Representative pictures of tumor immunostaining of leukocytes (CD45, red), monocytes (CD68, green), granulocytes (Gr-1, green), lymphocytes (CD4, green), and DAPI (blue). Scale bar, 100 (left panels) and 50  $\mu\text{m}$  (other panels). The number of CD45, CD68, Gr-1, and CD4 positive cells in tumor (n = 5-6). Data are presented as means  $\pm$  SEM.

## **2-6 Role of L-PGDS in vascular permeability and angiogenesis in mice inflammation model**

### **2-6-1 Role of L-PGDS in ear vascular hyper-permeability**

I determined if L-PGDS-PGD<sub>2</sub> signaling directly inhibits vascular permeability *in vivo*. Treatment with inflammatory stimulant croton oil (Oil, 2.5% in acetone, 3 h) or IL-1 $\beta$  (30 ng, 1 h) induced dye extravasation into the interstitium, and its leakage was observed in almost all parts of the ear (Fig. 29A upper panels). The L-PGDS<sup>-/-</sup> mice showed increase in vascular leakage compared to the WT mice (Fig. 29A, B), indicating exacerbation of vascular hyper-permeability.

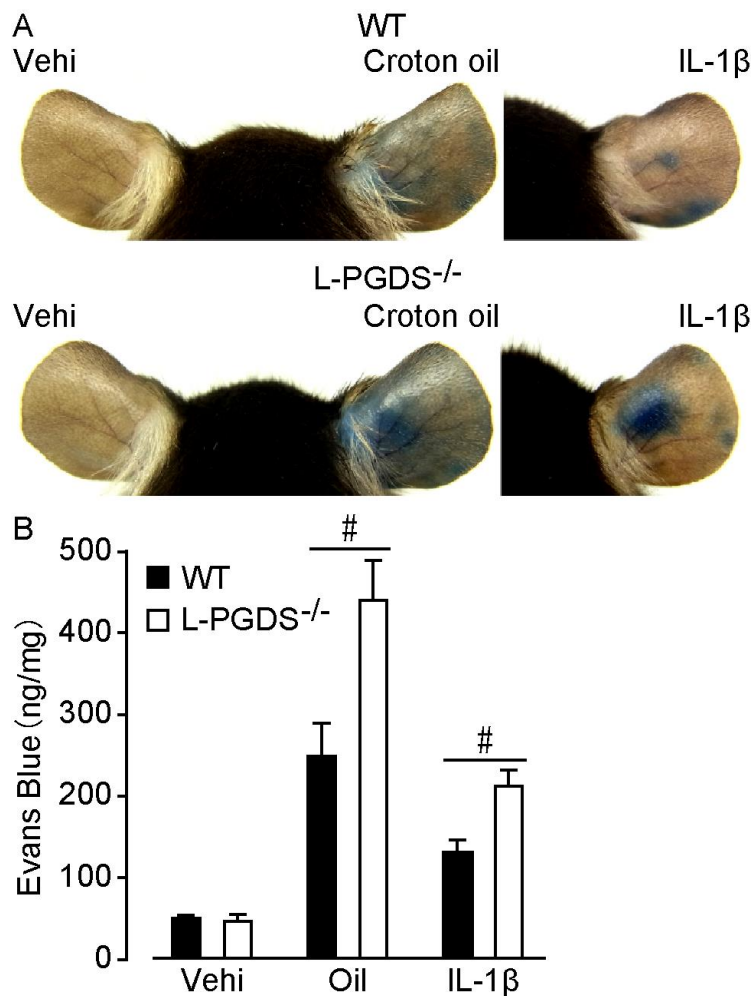


**Figure 29 L-PGDS deficiency exacerbated ear vascular hyper-permeability**

(A) Representative pictures of dye extravasation in the treatment with vehicle (left panels, left ear), croton oil (left panels, right ear), or IL-1 $\beta$  (right panels) in WT and L-PGDS<sup>-/-</sup> mice. (B) Quantification of dye extravasation in WT and L-PGDS<sup>-/-</sup> mice (n = 6). <sup>#</sup> Significantly different from the results in WT mice at p < 0.05. Data are presented as means  $\pm$  SEM.

### 2-6-2 L-PGDS localization in mice ear

Immunofluorescent staining of mice ear revealed that, consistent with the results in tumor ECs, L-PGDS was upregulated and localized in CD31 positive ECs by croton oil treatment (Fig. 30).

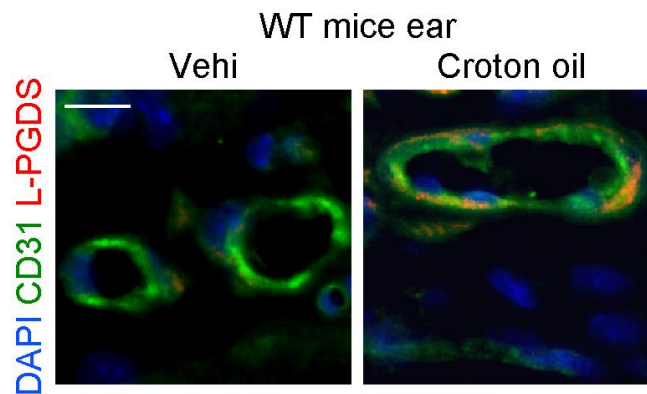


**Figure 30 L-PGDS was induced in EC of mice ear**

Representative pictures of mice ear immunostaining of DAPI (blue), CD31 (green), and L-PGDS (red) in vehicle- or croton oil-treated WT mice. Scale bar, 10  $\mu\text{m}$ .

### 2-6-3 Role of L-PGDS in cornea angiogenesis

I finally determine if L-PGDS-PGD<sub>2</sub> signaling inhibits angiogenesis *in vivo*. Implantations of pellets containing IL-1 $\beta$  (60 ng) and vascular endothelial growth factor (VEGF, 300 ng) in mice cornea induced angiogenesis from limbal vascular plexus to avascular areas within 6 days (Fig. 31A). L-PGDS<sup>-/-</sup> mice showed exacerbation of cornea neovascularization in response to these angiogenic stimuli compared to WT mice (Fig. 31A, B).

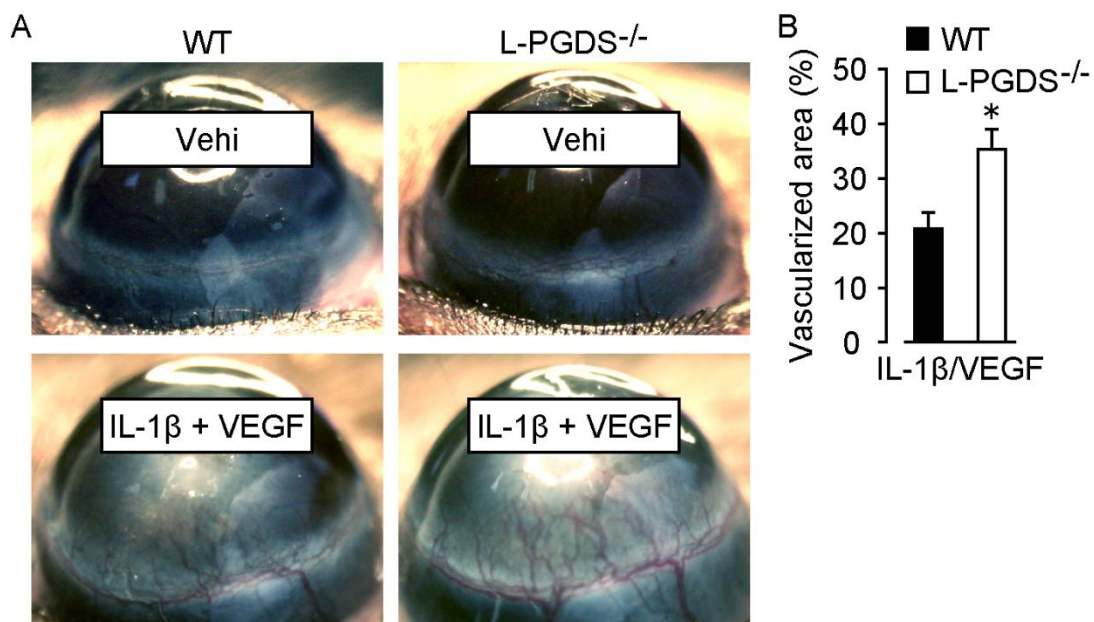


**Figure 31 L-PGDS deficiency exacerbated angiogenesis of mice cornea**

(A) Representative pictures of cornea angiogenesis in the treatment with vehicle (upper panels) or IL-1 $\beta$ - and VEGF (lower panels) in WT and L-PGDS<sup>-/-</sup> mice. (B) Quantification of cornea vascularized area (n = 6). \* Significantly different from the results in WT mice at p < 0.05. Data are presented as means  $\pm$  SEM.

## 2-7 Discussion of chapter 2

In the present chapter, I found that tumor cell-derived cytokine stimuli markedly increased the mRNA expression of L-PGDS in tumor ECs and that L-PGDS/PGD<sub>2</sub> axis acted as a negative feedback signaling against tumor growth by inhibiting vascular permeability, angiogenesis, and EndMT (Fig. 32).

There are several studies showing the pro-tumorigenic actions of tumor ECs. Amin *et al.* reported that tumor ECs isolated from human melanoma exhibited enhanced EGFR activation in response to EGF, leading to increased proliferative capability (39). Akiyama *et al.* also showed that high expression of P-glycoprotein accounted for drug resistance in human melanoma ECs (40). In contrast, this is the first study identifying anti-tumorigenic signaling pathway that can be activated in tumor ECs.

Prostaglandins are known as mediators of pro-inflammatory reactions that are responsible for exacerbation of several inflammation associated diseases, including cancers. PGE<sub>2</sub>, which is one of the main prostaglandins, is known to promote the growth of mice melanoma, breast tumor, or colorectal tumor by exacerbating tumor angiogenesis and tumor cell invasion (22). Another prostaglandin, thromboxane A<sub>2</sub> enhanced human prostate tumor cell motility, leading to poor prognosis (41). Epidemiologic studies revealed that routine use of COX-dependent prostaglandins syntheses inhibitors, nonsteroidal anti-inflammatory drugs (NSAIDs) inhibited the progression and prognosis of human colon cancer (18). In contrast to the established pro-inflammatory role of prostaglandins, Our group previously demonstrated that hematopoietic prostaglandin D synthase (H-PGDS)-derived PGD<sub>2</sub> from inflammatory cells has anti-inflammatory role in various mice models

including dermatitis (34), acute lung injury (33), and even cancer (38, 42). In detail, PGD<sub>2</sub> derived from neutrophil or mast cell H-PGDS acted on endothelial DP receptor, and ameliorated their symptoms by attenuating vascular permeability, angiogenesis, and inflammatory cell infiltration.

Although characters of tumor ECs have considered to be acquired by sustained inflammatory stimuli including cytokines and growth factors in tumor microenvironment (4, 43), its details were yet to be revealed (44). I here showed that tumor cell-derived IL-1 and TNF- $\alpha$  mainly elevated the mRNA expression of L-PGDS. Previous reports showed that several inflammatory cytokines such as IL-6 and TNF- $\alpha$  activates a transcription factor activator protein 1 (AP-1) in isolated ECs (45, 46), which induces L-PGDS mRNA transcription (47). Sustained exposure of cocktail of inflammatory cytokines or some specific cytokines but IL-1 and TNF- $\alpha$  in microenvironment may be responsible for the strong mRNA elevation of L-PGDS. Further investigations are needed to clarify this point.

Unlike previously known EndMT facilitating molecules (6, 48), PGD<sub>2</sub> is a unique endogenous molecule that inhibits EndMT in tumor. Recent study revealed that no less than 40% of cancer-associated fibroblasts, which exacerbate tumor malignancy, are converted by EndMT (7). Normalizing the tumor vessel might benefit to exclude these “evil” cells from the tumor. In the present study, I could not clarify the precise mechanism of PGD<sub>2</sub> in EndMT. PGD<sub>2</sub> possibly attenuates the expression of inflammatory cytokines or inhibits the TGF $\beta$  signal cascade itself (49). Further studies are needed to reveal the precise mechanisms of PGD<sub>2</sub> in EndMT.

As described above, there are only a few reports available from studies focusing on the role of L-PGDS in peripheral tissues instead of central nervous system. The present study showing their anti-tumorigenic role is the first one that demonstrates the pathophysiological contribution of L-PGDS-PGD<sub>2</sub> signaling in peripheral tissues. L-PGDS deficiency exacerbated both vascular permeability and angiogenesis in other peripheral inflammatory models; Miles assay and cornea angiogenesis assay as well as implanted tumor model. L-PGDS possibly represents anti-inflammatory reactions in various types of inflammation in peripheral tissues.

In this study, I focused on the role of L-PGDS in mice melanoma ECs. Unexpectedly, mRNA expression of L-PGDS was observed not only in ECs but also in some tumor cells of human melanoma. The melanoma-derived PGD<sub>2</sub> might negatively regulate tumor vascular permeability and angiogenesis, as well as EC-derived PGD<sub>2</sub>. I demonstrated that PGD<sub>2</sub> did not influence proliferation and survival of cultured B16F1 melanoma. However, there is still a possibility that PGD<sub>2</sub> somehow influence the tumorigenicity itself. Further studies are needed to clarify the precise role of L-PGDS-PGD<sub>2</sub> axis in respective tumor types.

In conclusion, I have identified L-PGDS-PGD<sub>2</sub> pathway as an anti-tumorigenic signaling pathway in tumor ECs. Tumor-derived cytokines upregulate mRNA expression of L-PGDS in ECs. The produced PGD<sub>2</sub> attenuates tumorigenic phenotype of tumor ECs by inhibiting vascular permeability, angiogenesis, and EndMT. Inhibition of tumorigenic transformation of ECs in tumor using this signal enhancement might be useful for future management of tumor malignancy (Fig. 32).

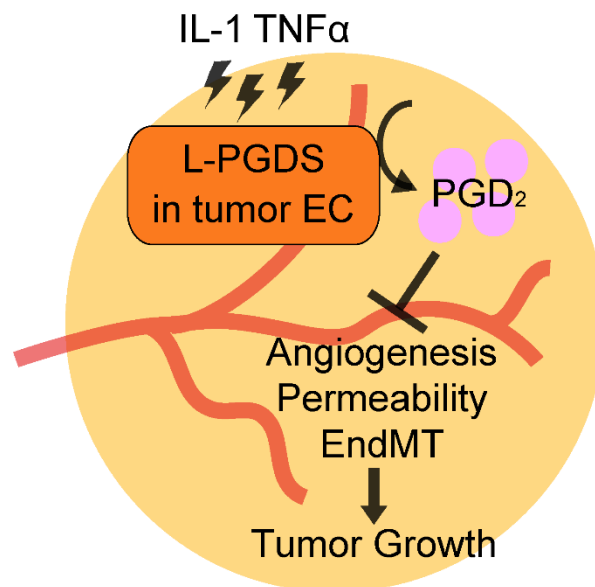


**Figure 32 The role of L-PGDS in tumor growth**

Tumor cell-derived IL-1 and TNF- $\alpha$  upregulated mRNA expression of L-PGDS in tumor ECs. L-PGDS produced PGD<sub>2</sub> and inhibited tumor angiogenesis, vascular permeability, and EndMT, leading to limit tumor growth.

## **Chapter 3 Role of PGD<sub>2</sub> in tumor metastasis**

本章の内容は、学術雑誌論文として出版する計画があるため公表できない。

5年以内に出版予定

## **Chapter 4 Total discussion**

本章の内容は、学術雑誌論文として出版する計画があるため公表できない。

5年以内に出版予定

## Chapter 5 Abstract

本章の内容は、学術雑誌論文として出版する計画があるため公表できない。

5年以内に出版予定

.

## **Chapter 6 Material and Methods**

本章の内容は、学術雑誌論文として出版する計画があるため公表できない。

5年以内に出版予定

## Chapter 7 Reference

1. McGuire S. World Cancer Report 2014. Geneva, Switzerland: World Health Organization, International Agency for Research on Cancer, WHO Press, 2015. *Adv Nutr.* 2016;7(2):418-9. Epub 2016/03/17.
2. Mehlen P, Puisieux A. Metastasis: a question of life or death. *Nature reviews Cancer.* 2006;6(6):449-58. Epub 2006/05/26.
3. Folkman J. Tumor angiogenesis: therapeutic implications. *The New England journal of medicine.* 1971;285(21):1182-6. Epub 1971/11/18.
4. Dudley AC. Tumor endothelial cells. *Cold Spring Harbor perspectives in medicine.* 2012;2(3):a006536. Epub 2012/03/07.
5. Denekamp J, Hobson B. Endothelial-cell proliferation in experimental tumours. *Br J Cancer.* 1982;46(5):711-20. Epub 1982/11/01.
6. Zeisberg EM, Potenta S, Xie L, Zeisberg M, Kalluri R. Discovery of endothelial to mesenchymal transition as a source for carcinoma-associated fibroblasts. *Cancer research.* 2007;67(21):10123-8. Epub 2007/11/03.
7. Potenta S, Zeisberg E, Kalluri R. The role of endothelial-to-mesenchymal transition in cancer progression. *Br J Cancer.* 2008;99(9):1375-9. Epub 2008/09/18.
8. St Croix B, Rago C, Velculescu V, Traverso G, Romans KE, Montgomery E, et al. Genes expressed in human tumor endothelium. *Science.* 2000;289(5482):1197-202. Epub 2000/08/19.
9. Seaman S, Stevens J, Yang MY, Logsdon D, Graff-Cherry C, St Croix B. Genes that distinguish physiological and pathological angiogenesis. *Cancer cell.* 2007;11(6):539-54. Epub 2007/06/15.
10. Waldhauer I, Steinle A. NK cells and cancer immunosurveillance. *Oncogene.* 2008;27(45):5932-43. Epub 2008/10/07.
11. Pluhar GE, Pennell CA, Olin MR. CD8(+) T Cell-Independent Immune-Mediated Mechanisms of Anti-Tumor Activity. *Critical reviews in immunology.* 2015;35(2):153-72. Epub 2015/09/10.
12. Li J, Jie HB, Lei Y, Gildener-Leapman N, Trivedi S, Green T, et al. PD-1/SHP-2 inhibits Tc1/Th1 phenotypic responses and the activation of T cells in the tumor microenvironment. *Cancer research.* 2015;75(3):508-18. Epub 2014/12/07.
13. Kitamura T, Qian BZ, Pollard JW. Immune cell promotion of metastasis. *Nature reviews Immunology.* 2015;15(2):73-86. Epub 2015/01/24.

14. Suzuki A, Leland P, Joshi BH, Puri RK. Targeting of IL-4 and IL-13 receptors for cancer therapy. *Cytokine*. 2015;75(1):79-88. Epub 2015/06/20.
15. Hodi FS, O'Day SJ, McDermott DF, Weber RW, Sosman JA, Haanen JB, et al. Improved survival with ipilimumab in patients with metastatic melanoma. *The New England journal of medicine*. 2010;363(8):711-23. Epub 2010/06/08.
16. Topalian SL, Hodi FS, Brahmer JR, Gettinger SN, Smith DC, McDermott DF, et al. Safety, activity, and immune correlates of anti-PD-1 antibody in cancer. *The New England journal of medicine*. 2012;366(26):2443-54. Epub 2012/06/05.
17. Ricciotti E, FitzGerald GA. Prostaglandins and inflammation. *Arteriosclerosis, thrombosis, and vascular biology*. 2011;31(5):986-1000. Epub 2011/04/22.
18. Chan AT, Ogino S, Fuchs CS. Aspirin use and survival after diagnosis of colorectal cancer. *Jama*. 2009;302(6):649-58. Epub 2009/08/13.
19. Harris RE. Cyclooxygenase-2 (cox-2) blockade in the chemoprevention of cancers of the colon, breast, prostate, and lung. *Inflammopharmacology*. 2009;17(2):55-67. Epub 2009/04/03.
20. Tsujii M, Kawano S, DuBois RN. Cyclooxygenase-2 expression in human colon cancer cells increases metastatic potential. *Proceedings of the National Academy of Sciences of the United States of America*. 1997;94(7):3336-40. Epub 1997/04/01.
21. Amano H, Hayashi I, Endo H, Kitasato H, Yamashina S, Maruyama T, et al. Host prostaglandin E(2)-EP3 signaling regulates tumor-associated angiogenesis and tumor growth. *J Exp Med*. 2003;197(2):221-32. Epub 2003/01/23.
22. Chang SH, Liu CH, Conway R, Han DK, Nithipatikom K, Trifan OC, et al. Role of prostaglandin E2-dependent angiogenic switch in cyclooxygenase 2-induced breast cancer progression. *Proc Natl Acad Sci U S A*. 2004;101(2):591-6. Epub 2003/12/23.
23. Ma X, Aoki T, Tsuruyama T, Narumiya S. Definition of Prostaglandin E2-EP2 Signals in the Colon Tumor Microenvironment That Amplify Inflammation and Tumor Growth. *Cancer research*. 2015;75(14):2822-32. Epub 2015/05/29.
24. Yang L, Huang Y, Porta R, Yanagisawa K, Gonzalez A, Segi E, et al. Host and direct antitumor effects and profound reduction in tumor metastasis with selective EP4 receptor antagonism. *Cancer research*. 2006;66(19):9665-72. Epub 2006/10/05.
25. Yamashita T, Sakuda K, Tohma Y, Yamashita J, Oda H, Irikura D, et al. Prostaglandin D synthase (beta-trace) in human arachnoid and meningioma cells: roles as a cell marker or in cerebrospinal fluid absorption, tumorigenesis, and calcification process. *J Neurosci*. 1997;17(7):2376-82. Epub 1997/04/01.
26. Qu WM, Huang ZL, Xu XH, Aritake K, Eguchi N, Nambu F, et al. Lipocalin-type prostaglandin D synthase produces prostaglandin D2 involved in regulation of physiological sleep. *Proc Natl Acad Sci U S A*. 2006;103(47):17949-54. Epub 2006/11/10.

27. Eguchi N, Minami T, Shirafuji N, Kanaoka Y, Tanaka T, Nagata A, et al. Lack of tactile pain (allodynia) in lipocalin-type prostaglandin D synthase-deficient mice. *Proc Natl Acad Sci U S A*. 1999;96(2):726-30. Epub 1999/01/20.
28. Taba Y, Sasaguri T, Miyagi M, Abumiya T, Miwa Y, Ikeda T, et al. Fluid shear stress induces lipocalin-type prostaglandin D(2) synthase expression in vascular endothelial cells. *Circ Res*. 2000;86(9):967-73. Epub 2000/05/16.
29. Matsuoka T, Hirata M, Tanaka H, Takahashi Y, Murata T, Kabashima K, et al. Prostaglandin D2 as a mediator of allergic asthma. *Science*. 2000;287(5460):2013-7. Epub 2000/03/17.
30. Nakamura T, Maeda S, Horiguchi K, Maehara T, Aritake K, Choi BI, et al. PGD2 deficiency exacerbates food antigen-induced mast cell hyperplasia. *Nature communications*. 2015;6:7514. Epub 2015/07/15.
31. Angeli V, Staumont D, Charbonnier AS, Hammad H, Gosset P, Pichavant M, et al. Activation of the D prostanoid receptor 1 regulates immune and skin allergic responses. *J Immunol*. 2004;172(6):3822-9. Epub 2004/03/09.
32. Hammad H, Kool M, Soullie T, Narumiya S, Trottein F, Hoogsteden HC, et al. Activation of the D prostanoid 1 receptor suppresses asthma by modulation of lung dendritic cell function and induction of regulatory T cells. *The Journal of experimental medicine*. 2007;204(2):357-67. Epub 2007/02/07.
33. Murata T, Aritake K, Tsubosaka Y, Maruyama T, Nakagawa T, Hori M, et al. Anti-inflammatory role of PGD2 in acute lung inflammation and therapeutic application of its signal enhancement. *Proceedings of the National Academy of Sciences of the United States of America*. 2013;110(13):5205-10. Epub 2013/03/13.
34. Sarashina H, Tsubosaka Y, Omori K, Aritake K, Nakagawa T, Hori M, et al. Opposing immunomodulatory roles of prostaglandin D2 during the progression of skin inflammation. *J Immunol*. 2014;192(1):459-65. Epub 2013/12/04.
35. Satoh T, Moroi R, Aritake K, Urade Y, Kanai Y, Sumi K, et al. Prostaglandin D2 plays an essential role in chronic allergic inflammation of the skin via CRTH2 receptor. *J Immunol*. 2006;177(4):2621-9. Epub 2006/08/05.
36. Muraki C, Ohga N, Hida Y, Nishihara H, Kato Y, Tsuchiya K, et al. Cyclooxygenase-2 inhibition causes antiangiogenic effects on tumor endothelial and vascular progenitor cells. *International journal of cancer*. 2012;130(1):59-70. Epub 2011/03/09.
37. Griffioen AW, Damen CA, Martinotti S, Blijham GH, Groenewegen G. Endothelial intercellular adhesion molecule-1 expression is suppressed in human malignancies: the role of angiogenic factors. *Cancer Res*. 1996;56(5):1111-17. Epub 1996/03/01.

38. Murata T, Lin MI, Aritake K, Matsumoto S, Narumiya S, Ozaki H, et al. Role of prostaglandin D2 receptor DP as a suppressor of tumor hyperpermeability and angiogenesis in vivo. *Proc Natl Acad Sci U S A*. 2008;105(50):20009-14. Epub 2008/12/09.
39. Amin DN, Hida K, Bielenberg DR, Klagsbrun M. Tumor endothelial cells express epidermal growth factor receptor (EGFR) but not ErbB3 and are responsive to EGF and to EGFR kinase inhibitors. *Cancer Res*. 2006;66(4):2173-80. Epub 2006/02/21.
40. Akiyama K, Maishi N, Ohga N, Hida Y, Ohba Y, Alam MT, et al. Inhibition of multidrug transporter in tumor endothelial cells enhances antiangiogenic effects of low-dose metronomic paclitaxel. *Am J Pathol*. 2015;185(2):572-80. Epub 2014/12/17.
41. Nie D, Guo Y, Yang D, Tang Y, Chen Y, Wang MT, et al. Thromboxane A2 receptors in prostate carcinoma: expression and its role in regulating cell motility via small GTPase Rho. *Cancer Res*. 2008;68(1):115-21. Epub 2008/01/04.
42. Murata T, Aritake K, Matsumoto S, Kamauchi S, Nakagawa T, Hori M, et al. Prostaglandin D2 is a mast cell-derived antiangiogenic factor in lung carcinoma. *Proceedings of the National Academy of Sciences of the United States of America*. 2011;108(49):19802-7. Epub 2011/11/23.
43. Motz GT, Santoro SP, Wang LP, Garrabrant T, Lastra RR, Hagemann IS, et al. Tumor endothelium FasL establishes a selective immune barrier promoting tolerance in tumors. *Nature medicine*. 2014;20(6):607-15. Epub 2014/05/06.
44. Kerbel RS. Tumor angiogenesis. *The New England journal of medicine*. 2008;358(19):2039-49. Epub 2008/05/09.
45. Delerive P, De Bosscher K, Besnard S, Vanden Berghe W, Peters JM, Gonzalez FJ, et al. Peroxisome proliferator-activated receptor alpha negatively regulates the vascular inflammatory gene response by negative cross-talk with transcription factors NF-kappaB and AP-1. *J Biol Chem*. 1999;274(45):32048-54. Epub 1999/11/05.
46. Lakshminarayanan V, Drab-Weiss EA, Roebuck KA. H2O2 and tumor necrosis factor-alpha induce differential binding of the redox-responsive transcription factors AP-1 and NF-kappaB to the interleukin-8 promoter in endothelial and epithelial cells. *J Biol Chem*. 1998;273(49):32670-8. Epub 1998/11/26.
47. Miyagi M, Miwa Y, Takahashi-Yanaga F, Morimoto S, Sasaguri T. Activator protein-1 mediates shear stress-induced prostaglandin d synthase gene expression in vascular endothelial cells. *Arterioscler Thromb Vasc Biol*. 2005;25(5):970-5. Epub 2005/02/19.
48. Rieder F, Kessler SP, West GA, Bhilocha S, de la Motte C, Sadler TM, et al. Inflammation-induced endothelial-to-mesenchymal transition: a novel mechanism of intestinal fibrosis. *Am J Pathol*. 2011;179(5):2660-73. Epub 2011/09/29.

49. Mihira H, Suzuki HI, Akatsu Y, Yoshimatsu Y, Igarashi T, Miyazono K, et al. TGF-beta-induced mesenchymal transition of MS-1 endothelial cells requires Smad-dependent cooperative activation of Rho signals and MRTF-A. *Journal of biochemistry*. 2012;151(2):145-56. Epub 2011/10/11.

## Acknowledgement

稿を終えるに際して、懇切なるご指導を賜りました東京大学大学院 放射線動物科学教室 村田 幸久 准教授、中村 達朗 特任助教に深甚なる謝意を表します。また様々な面でご協力を頂き、私の研究生活を支えてくださった研究室員や研究室 OB・OG の皆様に心から感謝いたします。最後に、本研究を進めるにあたり、犠牲となった多くの動物たちに心から感謝するとともに、その霊が慰められるよう心からお祈りいたします。